



Michigan Technological University  
Create the Future Digital Commons @ Michigan Tech

---

Dissertations, Master's Theses and Master's Reports - Open

Dissertations, Master's Theses and Master's Reports

---

2014

## DENSITY OF AMORPHOUS CARBON BY USING DENSITY FUNCTIONAL THEORY

Sorayot Chinkanjanarot  
*Michigan Technological University*

Follow this and additional works at: <https://digitalcommons.mtu.edu/etds>

 Part of the [Mechanical Engineering Commons](#)

Copyright 2014 Sorayot Chinkanjanarot

---

### Recommended Citation

Chinkanjanarot, Sorayot, "DENSITY OF AMORPHOUS CARBON BY USING DENSITY FUNCTIONAL THEORY", Master's report, Michigan Technological University, 2014.  
<https://digitalcommons.mtu.edu/etds/809>

Follow this and additional works at: <https://digitalcommons.mtu.edu/etds>

 Part of the [Mechanical Engineering Commons](#)

DENSITY OF AMORPHOUS CARBON  
BY USING DENSITY FUNCTIONAL THEORY

By

Sorayot Chinkanjanarot

A REPORT

Submitted in partial fulfillment of the requirements for the degree of

MASTER OF SCIENCE

In Mechanical Engineering

MICHIGAN TECHNOLOGICAL UNIVERSITY

2014

© 2014 Sorayot Chinkanjanarot



This report has been approved in partial fulfillment of the requirement for the Degree of MASTER OF SCIENCE in Mechanical Engineering.

Department of Mechanical Engineering – Engineering Mechanics

Report Advisor: *Dr. Gregory M. Odegard*

Committee Member: *Dr. John A. Jaszczak*

Committee Member: *Dr. Gowtham S*

Department Chair: *Dr. William W. Predebon*



## Table of Contents

<b>Table of Contents</b> .....	<b>v</b>
<b>List of Figures</b> .....	<b>vii</b>
<b>List of Tables</b> .....	<b>xi</b>
<b>Acknowledgments</b> .....	<b>xii</b>
<b>Abstract</b> .....	<b>xiii</b>
<b>Chapter 1: Introduction</b> .....	<b>1</b>
<b>Chapter 2: Background</b> .....	<b>4</b>
2.1 Introduction .....	4
2.2 Reactive Force Field .....	13
2.3 Density Functional Theory (DFT).....	14
<b>Chapter 3: Molecular Modeling and Position Refinement</b> .....	<b>16</b>
3.1 Preparation.....	16
3.2 Minimization and Position's Refinement by DFT .....	21
3.3 Visualization.....	32
<b>Chapter 4: Results and Discussion</b> .....	<b>35</b>
4.1 Density.....	35
4.2 Structure analysis.....	36
4.3 Energy analysis.....	48
<b>Chapter 5: Conclusion</b> .....	<b>51</b>
<b>Chapter 6: References</b> .....	<b>54</b>

<b>Appendix A</b> .....	<b>56</b>
A.1 Selection of Energy Cutoff and KPOINTS .....	56
A.2 Calculation of the standard deviation.....	58
<b>Appendix B: Computer Commands</b> .....	<b>59</b>
B.1 Unix Command .....	59
B.2 Computing Cluster.....	61
<b>Appendix C: Input files of LAMMPS (ReaxFF)</b> .....	<b>62</b>
C.1 script.coords .....	62
C.2 Imp_control.....	62
C.3 in.ac .....	63

## List of Figures

<i>Figure 1 Plot of the percentage <math>sp^3</math> bonding and the density of amorphous carbon, reprinted from P. J Fallon et al. (1993).....</i>	<i>5</i>
<i>Figure 2 Plot of comparison between theoretical RDF and experimental RDF by J. Kakinoki et al. (1960), reprinted from Galli et al. (1990) .....</i>	<i>7</i>
<i>Figure 3 Plot of <math>S(Q)</math> of TBMD (solid line) compared to experiment (dash line).....</i>	<i>8</i>
<i>Figure 4 Plot of RDF of TBMD (solid line) compared to experiment (dash line) of sample I and sample II, respectively.....</i>	<i>9</i>
<i>Figure 5 The overall procedure of this work that has three main parts: preparation, energy minimization and position refinement, and visualization.....</i>	<i>17</i>
<i>Figure 6 The first model of initial structure of amorphous carbon generated by random placement method .....</i>	<i>18</i>
<i>Figure 7 The first model of initial structure of amorphous carbon generated by liquid-quench method.....</i>	<i>20</i>
<i>Figure 8 The appearance of OVITO analyzing the first model of amorphous carbon created by the random placement method</i>	<i>33</i>
<i>Figure 9 The rendering process of OVITO analyzing the first model of amorphous carbon structure created by the random placement method .....</i>	<i>34</i>



<i>Figure 10 Shown the densities of amorphous carbon structures created by the random placement method and the liquid-quench method.....</i>	<i>35</i>
<i>Figure 11 The RDF plot of each final model of amorphous carbon created by the random placement method.....</i>	<i>36</i>
<i>Figure 12 Shown the bond order of the first final amorphous carbon model created by the random placement method with <math>sp^3</math> bonded atom red, <math>sp^2</math> green and <math>sp</math> blue.....</i>	<i>37</i>
<i>Figure 13 shown the bond order of the second final amorphous carbon model created by the random placement method with <math>sp^3</math> bonded atom red and <math>sp^2</math> green.....</i>	<i>38</i>
<i>Figure 15 shown the bond order of the third final amorphous carbon model created by the random placement method with <math>sp^3</math> bonded atom red and <math>sp^2</math> green.....</i>	<i>39</i>
<i>Figure 14 shown the bond order of the forth final amorphous carbon model created by the random placement method with <math>sp^3</math> bonded atom red, <math>sp^2</math> green and <math>sp</math> blue.....</i>	<i>39</i>
<i>Figure 16 shown the bond order of the fifth final amorphous carbon model created by the random placement method with <math>sp^3</math> bonded atom red, <math>sp^2</math> green and <math>sp</math> blue.....</i>	<i>40</i>
<i>Figure 17 shown the RDF plot of each final model of amorphous carbon created by the liquid-quench method .....</i>	<i>41</i>

*Figure 18 shown the bond order of the first final amorphous carbon model created by the liquid-quench method with  $sp^3$  bonded atom red and  $sp^2$  green.....42*

*Figure 19 shown the bond order of the second final amorphous carbon model created by the liquid-quench method with  $sp^3$  bonded atom red,  $sp^2$  green and  $sp$  blue.....42*

*Figure 20 shown the bond order of the third final amorphous carbon model created by the liquid-quench method with  $sp^3$  bonded atom red,  $sp^2$  green and  $sp$  blue.....43*

*Figure 21 shown the bond order of the forth final amorphous carbon model created by the liquid-quench method with  $sp^3$  bonded atom red,  $sp^2$  green and  $sp$  blue.....44*

*Figure 22 shown the bond order of the fifth final amorphous carbon model created by the liquid-quench method with  $sp^3$  bonded atom red,  $sp^2$  green and  $sp$  blue.....44*

*Figure 23 shown the average percentages of each bond order of the final amorphous carbon models by using OVITO.....45*

*Figure 24 compared the average  $sp^3$  percentage of amorphous carbon created by both methods using OVITO and Equation 1 .....46*

*Figure 25 compared average RDF of amorphous carbon structure created by the random placement method and the liquid-quench method .....47*

*Figure 26 shown the ground-state energies of amorphous carbon structure generated by both methods changing by the ionic step ..... 48*

*Figure 27 shown the densities of amorphous carbon structure generated by both methods changing by the ionic step..... 49*

*Figure 28 compared the ground energies of amorphous carbon by changing energy cutoff variable ..... 56*

## List of Tables

<i>Table 1 shown all combination of ISIF parameters.....</i>	<i>22</i>
<i>Table 2 shown all descriptions of ISMEAR parameters.....</i>	<i>23</i>
<i>Table 3 shown all description of IBRION parameters.....</i>	<i>25</i>
<i>Table 4 shown the comparison the densities between this present work and the previous literatures.....</i>	<i>53</i>
<i>Table 5 shown the ground energies of amorphous carbon structure by varying KPOINTS and energy cutoff.....</i>	<i>57</i>
<i>Table 6 shown the unix commands used in this work.....</i>	<i>59</i>

## **Acknowledgments**

I would like to sincerely thank Dr. Gregory Odegard for mentoring me; to Dr. Kristopher Wise and Dr. Benjamin Jensen at NASA Langley Research Center for their advice; to Dr. John Jaszczak and Dr. Gowtham S for being the committee; to Matthew Radue for showing me how to render the pictures. Finally, I am really grateful to my family for their support and cheer.

This research is funded by NASA Langley Research Center under grant NNX09AM50A.

## Abstract

Amorphous carbon has been investigated for a long time. Since it has the random orientation of carbon atoms, its density depends on the position of each carbon atom. It is important to know the density of amorphous carbon to use it for modeling advance carbon materials in the future. Two methods were used to create the initial structures of amorphous carbon. One is the random placement method by randomly locating 100 carbon atoms in a cubic lattice. Another method is the liquid-quench method by using reactive force field (ReaxFF) to rapidly decrease the system of 100 carbon atoms from the melting temperature. Density functional theory (DFT) was used to refine the position of each carbon atom and the dimensions of the boundaries to minimize the ground energy of the structure. The average densities of amorphous carbon structures created by the random placement method and the liquid-quench method are 2.59 and 2.44 g/cm<sup>3</sup>, respectively. Both densities have a good agreement with previous works. In addition, the final structure of amorphous carbon generated by the liquid-quench method has lower energy.



## Chapter 1: Introduction

Carbon<sup>1</sup> is a very important element on the earth. It was discovered and used for a long time in the form of soot, charcoal, graphite, and diamond. In the past, these forms were considered to be different elements. Carbon was been known in the form of charcoal in prehistoric time. Carbon is from the word from Latin that means burnt wood as "Carbo."

It is claimed that diamond was discovered in India at least 3000 years ago. In 1772, Antoine Lavoisier, a French scientist, burned charcoal and the diamond by magnifying sun light on them. He found that both things had the same amount of carbon dioxide gas per gram. So, this became the conclusion that the charcoal and the diamond are the same element.

In the past, graphite was named black lead or "Plumbago", which means "lead" in Latin, because people did not distinguish graphite from lead. Until 1779, a Swedish scientist named Carl Wilhelm Scheele proved that the graphite is another form of carbon by burning graphite to be carbon dioxide. In 1796, Smithson Tennant, an English chemist, showed that carbon is not only part of the diamond but the diamond is a pure carbon. He proved this by burning same weighted quantities of charcoal and diamond to become only carbon dioxide. Both materials transformed to be equal quantity of carbon dioxide gas. In 1855, pure graphite



was created from carbon by Benjamin Brodie, an English chemist. He concluded that graphite is a form of carbon.

In the 1967 World's fair, an architect named Buckminster Fuller designed the geodesic domes. Then, in 1985, Harold Kroto and Robert Carl, Jr. discovered a new form of carbon that its geometry looks like the geodesic domes. So, it has been called "buckminsterfullerene."

In 1991, carbonnanotubes were discovered in the soot by Sumio Iijima, a Japanese physicist at the Nippon Electronic Company, Limited (NEC). From this discovery, there were many later research projects about carbon nanotubes. Nowadays, carbon nanotube network materials have become more popular due to thier unique properties.

Graphene<sup>2</sup> has recently been very interested materials. In 2010, Andre K. Geim and Konstantin S. Novoselov obtained noble prize in Physics from the paper about the graphene that published in 2004. Graphene is the single-layer of carbon atoms located in hexagonal lattice. Their properties are electrically conductive, mechanically strong, transparent, and flexible. In 2010, Andre K. Geim and Konstantin S. Novoselov obtained noble prize in Physics from the paper that published in 2004.

Amorphous carbon was introduced to the world more than five decades ago. Since each carbon atom oriented randomly, amorphous carbon has become a material

of interest in the scientific community. There were many experimentally and computationally researches about the amorphous carbon.

Amorphous carbon has also been an important material in future aerospace structures because of its ability to act as a binder in carbon nanotube network materials. These materials are lightweight, strong, and electrically conductive. Little is known about the molecular structure of amorphous carbon, which inhibits research in carbon nanotube network materials.

## Chapter 2: Background

### 2.1 Introduction

Amorphous carbon has widely been investigated in experimental and computational research. Due to the disordered nature of this phase of carbon, the density and hybridization of amorphous carbon is being determined by many methods.

Many experiments attempted to describe the properties of amorphous carbon. In 1960, J. Kakinoki et al.<sup>3</sup> used electron diffraction to study thin carbon film in amorphous state. The density of the specimen was needed for this research. It was determined by measuring thickness, cross-section area, and weight that was measured by a quartz torsion balance. Then, the density was calculated to be equal to 2.4 g/cm<sup>3</sup>. In 1968, B. T. Boiko et al.<sup>4</sup> also determined the properties of amorphous carbon. They obtained the density to be equal to 2.1 g/cm<sup>3</sup>.

In 1984, D. Beeman et al.<sup>5</sup> created the modeling of amorphous carbon by hand. They created four models of amorphous carbon structures from the previous experiments. Model C1120 contained 1120 carbon atoms with all threefold bonding. The density of this model was equal to 2.11 g/cm<sup>3</sup>. Moreover, the other three models: C340, C356, and C519 showed that their densities were equal to 2.69, 3.21, and 3.39 g/cm<sup>3</sup>, respectively. The bonding of the model C519 was all four-fold.

Li and Lannin<sup>6</sup> obtained the radial distribution function (RDF) of amorphous carbon film by using neutron diffraction in 1990. The density of amorphous carbon was determined by this RDF to be 2.44 g/cm<sup>3</sup>. Three years later, P. J. Fallon et al.<sup>7</sup> created amorphous carbon films by cathodic carbon arc from filtered ion beams. Then, Rutherford backscattering spectroscopy (RBS) and surface profilometer were used to find the density area and the thickness, respectively. The density of amorphous carbon was calculated by dividing the density area by the thickness that was in the range of 2.25 to 2.9 g/cm<sup>3</sup>. Electron energy loss spectroscopy (EELS) was performed to determine the sp<sup>3</sup> fraction. The sp<sup>3</sup> fractions of these amorphous carbon films is shown in *Figure 1* regarding to the density. As it shown, the maximum sp<sup>3</sup> fraction is 80%.

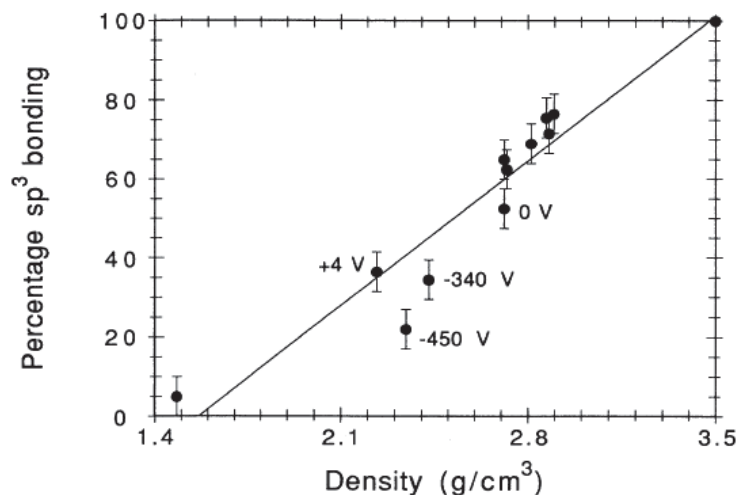


*Figure 1* Plot of the percentage sp<sup>3</sup> bonding and the density of amorphous carbon, reprinted from P. J Fallon et al. (1993)

Another three years later, G. M. Pharr et al.<sup>8</sup> produced amorphous carbon films on silicon prepared by cathodic-arc deposition with substrate pulse biasing. The density of these amorphous carbon films was calculated from the results from

RBS and surface profilometer. The range of the density was from 2.14 to 3.00 g/cm<sup>3</sup>. The sp<sup>3</sup> fraction was from 39% to 85% by using EELS.

In 1999, A.C. Ferrari et al.<sup>9</sup> used an S-bend filtered cathodic vacuum arc (FCVA) on Si wafers at ion energy of 100 eV to deposit the tetrahedral amorphous carbon. By using EELS and X-ray reflection (XRR), the sp<sup>3</sup> fraction was 88% and the density was calculated to be equal to 3.26 g/cm<sup>3</sup>, respectively. One year later, A.C. Ferrari with a different research team<sup>10</sup> generated tetrahedral amorphous carbon films by using single-bend FCVA at -80 V that the density was equal to 3.20 g/cm<sup>3</sup> derived by XRR and from plasmon energies. Each sp<sup>3</sup> fraction of amorphous carbon films was determined by using EELS. The relationship between sp<sup>3</sup> fraction and the density of amorphous carbon was a linear fit shown in *Equation 1*. The sp<sup>3</sup> fraction was equal to 100% when the density was about 3.3 g/cm<sup>3</sup>.

$$\rho \text{ (g/cm}^3\text{)} = 1.92 + 1.37(\text{sp}^3\text{ fraction)} \quad \text{Equation 1}$$

In 2002, Masaya Iwaki<sup>11</sup> concluded that the atomic density of amorphous carbon was from 2.0 to 2.3 g/cm<sup>3</sup>. The diamond-like carbon (DLC) was deposited on the silicon wafers by using physical vapor deposition (PVD) method with a benzene gas source. The density was calculated from the depth of implanted element measured by secondary ion mass spectrometry (SIMS) and the density area distribution determined by RBS. This sample used the implanted element as a marker.

Computational chemistry has widely become a tool to study and understand the properties of materials at the molecular level. In 1988 J. Tersoff<sup>12</sup> introduced an empirical method to describe the structural properties of carbon. Two samples were created by condensing the vapor and quenching the liquid. Respective densities were 2.18 and 2.39 g/cm<sup>3</sup>. These densities were met close to the experimental densities that were from 1.40 to 2.11 g/cm<sup>3</sup> summarized by J. Robertson<sup>13</sup> in 1986. Then, in 1990, G.Galli et al.<sup>14</sup> determined the properties of amorphous carbon by using Ab initio calculation or the first-principles molecular dynamics. The structure of 54 carbon atoms with periodic-boundary condition was set into molecular dynamics (MD) simulation by fixing the density of 2.0 g/cm<sup>3</sup>. The result of this work was a good agreement with most results of experiment at that time. *Figure 2* shows that both the results from the simulation and the experiment by J. Kikanoki et al.

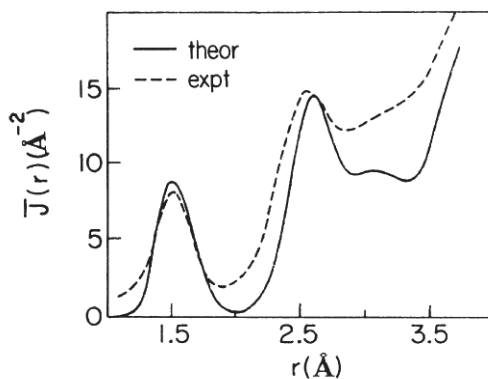


*Figure 2* Plot of comparison between theoretical RDF and experimental RDF by J. Kakinoki et al. (1960), reprinted from Galli et al. (1990)

In 1993, C. Z. Wang et al.<sup>15</sup> performed tight-binding molecular dynamics (TBMD) for studying the structural and electrical properties of amorphous carbon. The amorphous carbon structure was created by the liquid-quenching method with 216 carbon atoms. The densities of amorphous carbon structures were 2.20, 2.44, and 2.69 g/cm<sup>3</sup>. They obtained a structure factor  $S(Q)$  in good agreement with neutron diffraction on amorphous carbon films by Li and Lannin in 1990 shown in *Figure 3*.

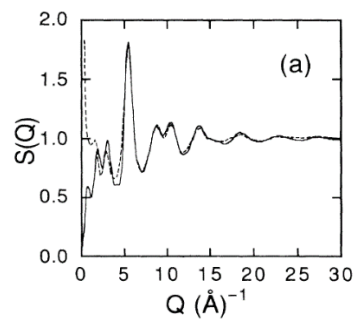


*Figure 3* Plot of  $S(Q)$  of TBMD (solid line) compared to experiment (dash line)

One year later, C. Z. Wang and K. M. Ho<sup>16</sup> studied more about the diamond-like amorphous carbon. Two samples were generated by using the quenching method. Their densities were equal to 3.35 and 3.40 g/cm<sup>3</sup>. In both papers, the summary of the density amorphous carbon is from 2.20 to 3.40 g/cm<sup>3</sup>. *Figure 4*

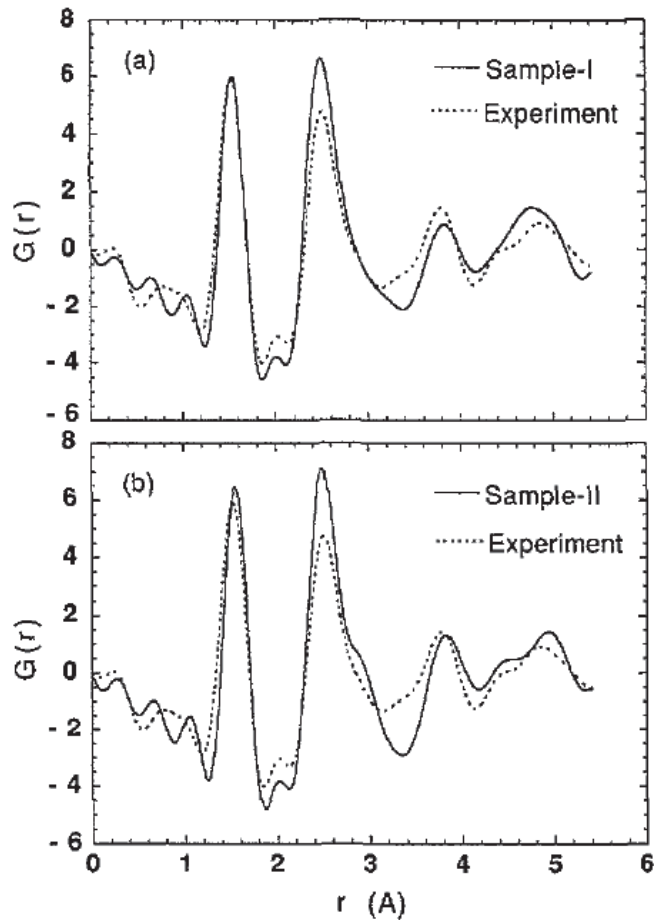


Figure 4 Plot of RDF of TBMD (solid line) compared to experiment (dash line) of sample I and sample II, respectively

In 1996, N. A. Mark et al.<sup>17</sup> used Car-Parrinello first-principles molecular-dynamics to simulate the tetrahedral amorphous carbon network. The result was in good agreement with the experimental result at the density of 3 g/cm<sup>3</sup>. The sp<sup>3</sup> and sp<sup>2</sup> fraction were 65% and 35%, respectively. Six years later, K. Kohary and S. Kugler<sup>18</sup> used TBMD to study six different amorphous carbon networks. The sample was created by growing the amorphous carbon thin films on a



diamond surface. The density of amorphous carbon at substrate temperature of 100 K was from 2.4 to 3.0 g/cm<sup>3</sup> and at substrate temperature of 300 K was from 2.0 to 2.3 g/cm<sup>3</sup>.

In 2005, M. G. Fyta et al.<sup>19</sup> showed the relationship between the density and sp<sup>3</sup> fraction of amorphous carbon from previous work. The range of density was 1.3 to 3.3 g/cm<sup>3</sup>. Moreover, TBMD and Monte Carlo (MC) were used to investigate the properties of nanocomposite carbon. The matrix of this composite material was amorphous carbon. They concluded that the nanocomposite carbon is stable if the sp<sup>3</sup> fraction of amorphous carbon matrices is above 60% that can be derived to be the density by using *Equation 1*. The density of matrices should be above 2.8 g/cm<sup>3</sup>.

In 2013, Longqiu Li et al.<sup>20</sup> generated amorphous carbon with density from 2.0 to 3.2 g/cm<sup>3</sup> by using the liquid-quench method in MD. Three empirical potential functions: the reactive force field (ReaxFF), the second generation of the reactive bond order (2<sup>nd</sup> REBO), and the Tersoff potential were used for the simulations. They concluded that the 2<sup>nd</sup> REBO can be performed well for a smaller density of 2.4 g/cm<sup>3</sup>. The ReaxFF was good if the density of amorphous carbon was below 2.6 g/cm<sup>3</sup>. Finally, the Tersoff is recommended to use for the diamond-like tetrahedral amorphous carbon.

From previous works, amorphous carbon has been studied and investigated by the experiments and the computer simulations for over half a century. The

properties of amorphous carbon were varied by the environments in each study. At the beginning, the density of amorphous carbon from the experiment was quite low as the review from J. Robertson in 1986. There is an assumption that the samples might have the air inside the structure making voids so this perhaps is the reason for the small density. Many years later, the samples were prepared appropriately by implementing the theoretical models and the measurement was much more accurate. Moreover, it was also the beginning of the computer simulations that can roughly predict the results to eliminate the unnecessary experiments. Most results for the density of amorphous carbon in this period was in the range between graphite and diamond densities that are 2.26 and 3.51 g/cm<sup>3</sup>.

High-performance computer simulation has been frequently used to determine the properties of amorphous carbon recently. The remarkable work of Longqiu Li et al. in 2013 that they used ReaxFF to calculate the structural properties of amorphous carbon is very interesting and ReaxFF is now widely used to simulate the carbon-based materials. To determine the density of amorphous carbon in a stable state, DFT is an excellent tool to minimize the local energy by allowing the atoms and the volume of the structure to be changed.

Since the combination of simulations between ReaxFF and DFT has not yet been used to find the density of amorphous carbon, it is interesting to generate the random structure of amorphous carbon with ReaxFF by using the liquid-quench method. Then, the initial amorphous carbon structure is optimized with DFT for

minimizing the energy and refining the position of amorphous carbon. This process can provide the complete random structure at the beginning and produce the lowest-energy amorphous carbon structure. Moreover, another modeling method is performed to generate the initial structure that is the random placement carbon atoms on a cubic lattice. The structures of both random placement method and liquid-quench method are determined for the densities and the  $sp^3$  fractions of their structures. They are also compared the results together to see the differences.

## **2.2 Reactive Force Field**

Reactive Force Field (ReaxFF)<sup>21</sup> was designed to simulate the large scale reactive chemical system. At the beginning, ReaxFF was developed to model the bond dislocation and formation for hydrocarbons. ReaxFF is regarded to the relationship between bond distance and bond order and also the relationship between bond order and bond energy. ReaxFF can perform non-bonding interactions between all atoms since Coulomb and van der Waals potentials are included. The potential is defined as a function of bond order with energy penalties. Moreover, the parameters were derived from quantum chemical calculations on bond dissociation and reaction of small molecule of formation and geometry data of stable carbon-based materials.

ReaxFF was used to model amorphous carbon by using the liquid-quench method. ReaxFF has the ability to generate amorphous carbon that has density below 2.6 g/cm<sup>3</sup> that its sp<sup>3</sup> fraction was good agreement with the sp<sup>3</sup> of amorphous carbon calculated by DFT. In contrast, ReaxFF was unsuitable to predict the sp<sup>3</sup> fraction of tetrahedral amorphous carbon that its density was from 2.6 g/cm<sup>3</sup> and above.

### **2.3 Density Functional Theory (DFT)**

Density Functional Theory (DFT)<sup>22</sup> is the computational quantum mechanical modeling technique that can be used to accurately determine the equilibrium molecular structure of complex materials. The word of density means the density of electron of structure and functional means the function of the function that the example is shown in *Equation 2*.

$$F(f(x)) = \int_0^1 f(x)dx \quad \text{Equation 2}$$

This is a function of the function  $f(x) = x + 1$ , the solution of this example is 2.

There are many levels of calculation that depends on the exchange-correlation functional. At the beginning, the nuclei were fixed and the electrons were described by using the local density approximation (LDA)<sup>23</sup>. After that the generalized gradient approximation (GGA) was developed that included more information than LDA. Two functionals of GGA that have mostly been used are the Perdew-Wang functional (PW91)<sup>24,25</sup> and the Perdew-Burke-Ernzerhof functional (PBE)<sup>26,27</sup>. Moreover, the plane-wave DFT is another type of DFT that can be performed efficiently.

Plane-wave DFT has now become popular as a computational tool to study and predict the solution of engineering problems. It is very good to model the crystal structure or the solid bulk system. Plane-wave basis required the pseudopotentials for computing the simulation. This basis set is not expensive compared to the other basis set.

K-point is the parameter to define the accuracy of the simulation but this must be considered with the simulation's time. K-point has to be indicated in three dimensions as an initial parameter. Furthermore, the energy cutoff is also necessary for the simulation depending on type of materials that should also be set in the input file.

## **Chapter 3: Molecular Modeling and Position Refinement**

This chapter describes the procedure to determine the density of amorphous carbon. Three main parts are introduced: preparation, energy minimization and position's refinement, and visualization shown in *Figure 5*.

### **3.1 Preparation**

This part shows the steps to generate the initial structures of amorphous carbon by using random placement of carbon atoms on a cubic lattice and liquid-quench method.

For random placement of carbon atoms on a cubic lattice, 100 carbon atoms were positioned randomly in a large cubic lattice. The length of each side of the cube was set depending on the density of initial amorphous carbon structure. Since the initial density was established at  $3 \text{ g/cm}^3$ , the length was equal to the cube root of volume of the cube that was  $8.7268 \text{ \AA}$ . This cube was portioned to be 5 spaces on each side so there were 125 spaces. Then, each carbon atom was randomly located into 100 spaces. This became the initial structure of amorphous carbon

Next, energy minimization was contestant. For consistency of the result, five models were generated for repeating simulation. The first model of this method is shown in *Figure 6*.

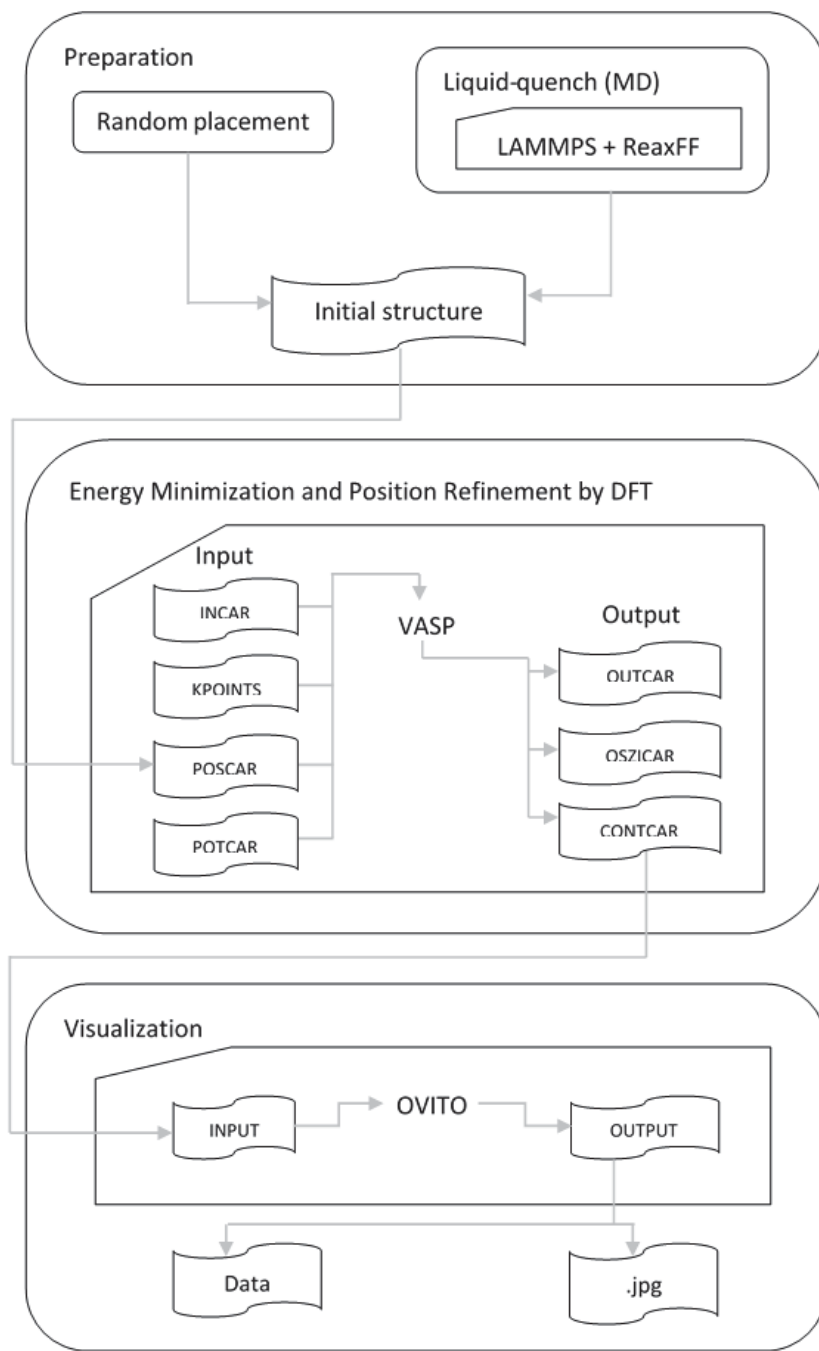
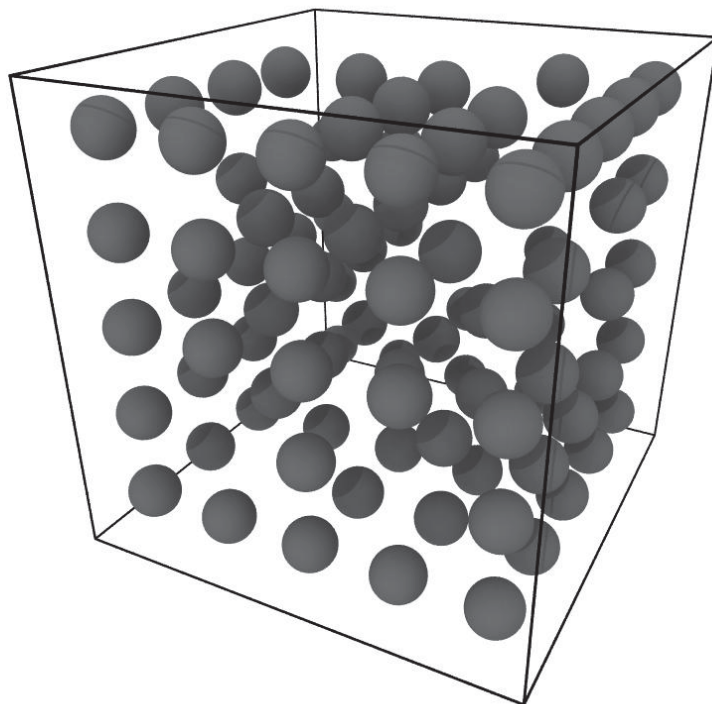


Figure 5 The overall procedure of this work that has three main parts: preparation, energy minimization and position refinement, and visualization





*Figure 6 The first model of initial structure of amorphous carbon generated by random placement method*

There were two different densities of amorphous carbon structure that were also created by the random placement method. They are 1.0 and 2.0 g/cm<sup>3</sup>. At the beginning, all three different densities were initial optimized by DFT. When the simulation were finished, all structures of amorphous carbon approached to the density of 2.6 g/cm<sup>3</sup>.

For the liquid-quench method, the carbon atoms were randomly placed into a molecular dynamics simulation box (ReaxFF) by using random function at the density of 2.6 g/cm<sup>3</sup>. By changing the seed number in random function, this

method can generate the amorphous carbon for the other different models. At the beginning, this structure was simulated with the atomic motion at 5000 K. The temperature of the simulation box was rapidly reduced to 1 K with the time span at 500 femtoseconds (fs). NVE was used in this modeling: N means constant number of atoms, V means constant volume, and E means constant energy. This simulation's time was 100 picoseconds (ps). The version of Reaxff used in this work was the Reactive MD-force field: June 18 2013 c/h/o.

When the simulation was done, all positions of the carbon atom of each time step were written to the output file by using the dump command. The data of simulation was written every 1 ps to the dump and output files. The position of each carbon atom was selected from the final time step. The first model of the liquid-quench method was shown *in Figure 7*.

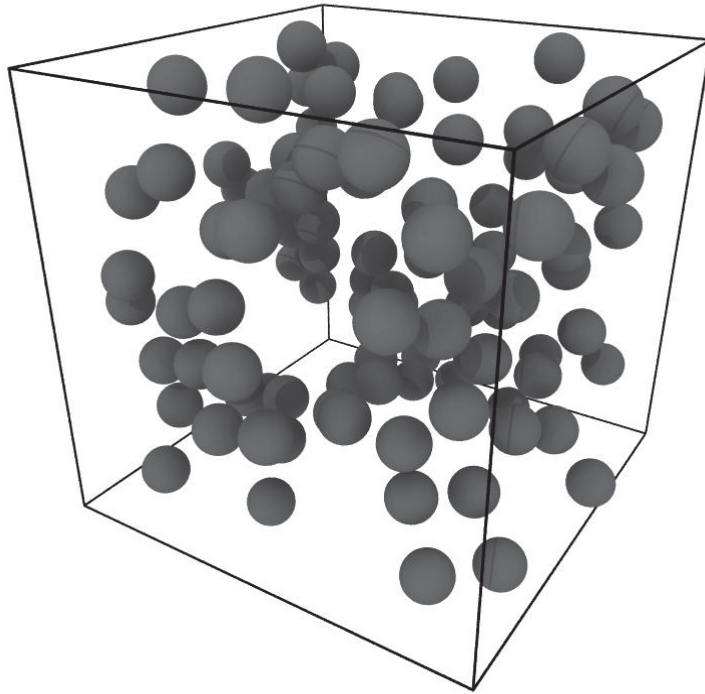


*Figure 7 The first model of initial structure of amorphous carbon generated by liquid-quench method*

### **3.2 Minimization and Position's Refinement by DFT**

The Vienna Ab initio Simulation Package (VASP)<sup>28-31</sup> was used to minimize the energy of amorphous structures. VASP is good for the crystal structure with plane-wave DFT. It is also able to move carbon atoms in each step and to change the volume of the structure. Four input files are necessary to submit the simulation including parameters and command that are INCAR, KPOINTS, POSCAR, and POTCAR.

**INCAR** contains basic parameters to run the simulation. The sample of INCAR file including the details is shown in the following.

---

```
SYSTEM      = Amorphous_carbon
ENCUT       = 600          #Energy cut-off
ISIF        = 3           #Allows the cell and ions to fully relax
ISMEAR      = 0           #Guassian Smearing
SIGMA       = 0           #Smearing width in eV
LPLANE      = .TRUE.
NPAR        = 4           #Distribute band calculations on all processors
LSCALU      = .FALSE.
NSIM        = 4
PREC        = high        #Precision high
LREAL       = Auto        #Automatically select projection operators
NSW         = 100         #Number of ionic steps
IBRION      = 1           #RMM-DIIS algorithm for ion relaxation
EDIFF       = 1e-8
EDIFFG      = -0.0001
```

---

**ENCUT** indicates the cutoff energy for the plane wave basis in the electron volt (eV) unit. The default of this parameter is the largest ENMAX in the POTCAR file. The simulation includes all plane waves where the kinetic energy is smaller than

ENCUT into the basis set. The cutoff energy of 600eV was chosen and set to all simulations in this work. The method of selection is shown in Appendix A.

**ISIF** controls whether the stress tensor is calculated and which degrees-of-freedom are allowed to change in the relaxation and MD run. The degrees-of-freedom include ionic positions, cell volume, and cell shape. All combinations of the degrees-of-freedom and the stress tensor are shown in *Table 1*. ISIF of 3 was chosen to allow all degrees of freedom change to compute updated density of amorphous carbon.

*Table 1 shown all combination of ISIF parameters*

ISIF	Forces	Stress tensor	Degrees of freedom		
			Positions	Cell shape	Cell Volume
0	Yes	No	Yes	No	No
1	Yes	Trace only	Yes	No	No
2	Yes	Yes	Yes	No	No
3	Yes	Yes	Yes	Yes	Yes
4	Yes	Yes	Yes	Yes	No
5	Yes	Yes	No	Yes	No
6	Yes	Yes	No	Yes	Yes
7	Yes	Yes	No	No	Yes

**ISMEAR** determines how the partial occupancies are set for each orbital. The description of each integer for indicating ISMEAR is shown in *Table 2*. ISMEAR of 0 was selected to use Gaussian smearing.

*Table 2 shown all descriptions of ISMEAR parameters*

<b>ISMEAR</b>	<b>Type of smearing</b>
N (N > 0)	Method of Methfessel-Paxton order N
0	Gaussian smearing
-1	Fermi smearing
-2	Partial occupancies are read from the WAVECAR an INCAR file, and kept fixed throughout run
-3	Perform a loop over smearing parameters supplied in the INCAR file
-4	Tetrahedral method using a $\Gamma$ -centered k-mesh
-5	Tetrahedral method with Blöchl corrections using a $\Gamma$ -centered k-mesh

**SIGMA** specifies the width of the smearing in eV. SIGMA was set to be 0 in this work.

**LPLANE** switches on the plane-wise data distribution in real space. This parameter was set to be ".TRUE." for which combination of NPAR and LPLANE can be used and the data distribution in real space is done in plane wise.

**NPAR** determines the number of bands that are treated in parallel. Since VASP 5.3.3, which this research has been used, includes the parallelization and data distribution over bands and/or over plane wave coefficient, this parameter is necessary to be appropriately specified to number of cores of computing cluster. NPAR is strongly recommended to set as the square root of number of cores for multi-core machines. Each simulation used 16 cores of the processors so NPAR was set to be 4.

**LSCALU** switches on the parallel LU decomposition in the orthonormalization of the wave functions. This parameter was set to be ".FALSE." as the default.

**NSIM** sets the number of bands that are optimized simultaneously by the RMM-DIIS algorithm. NSIM was set equal to 4 as the default.

**PREC** specifies the precision mode. PREC was set to "high".

**LREAL** determines whether the projection operators are calculated in real-space or in reciprocal space. LREAL was set to be "Auto". The projection is done in real space and fully automatically optimizes projection operators.

**NSW** sets the maximum number of ionic steps by integer. NSW was equal to 100.

**IBRION** controls how the ions are updated and move. *Table 3* shows the description of each number of IBRION which was set equal to 1 (RMM-DIIS algorithm).

*Table 3 shown all description of IBRION parameters*

<b>IBRION</b>	<b>Description</b>
-1	No update
0	Molecular Dynamics
1	Ionic relaxation (RMM-DIIS algorithm)
2	Ionic relaxation (conjugate gradient algorithm)
3	Ionic relaxation (damped molecular dynamics)
5 and 6	Second derivatives, Hessian matrix and phonon frequencies (finite differences)
7 and 8	Second derivatives, Hessian matrix and phonon frequencies (perturbation theory)
44	The improved Dimer Method

**EDIFF** specifies the global break condition for the electronic SC-loop, it was set equal to  $1e-8$ .

**EDIFFG** specifies the break condition for the ionic relaxation loop, it was set equal to  $-0.0001$ .



**KPOINTS** set k-point number or mesh size of the grid for calculation. There are two types of KPOINTS: the entering all k-points explicitly and the automatic k-mesh generation. The second method was selected for this work. An example of KPOINTS file was used in this work shown below.

---

Automatic mesh

```
0                ! number of k-points = 0 ->automatic generation scheme
Monkhorst-Pack   ! select Monkhorst-Pack (first letter is significant)
5 5 5           ! size of mesh (5x5x5 points along b1, b2, b3)
0. 0. 0.        ! shift of the k-mesh
```

---

The first line is the comment line. The second line must set to be smaller or equal to 0 for defining to be automatic meshing. For the third line, there are two type of the mesh. One is the original Monkhorst-Pack using this by indicating "M" or "m" on the first letter of this line. Another type was indicated by "G" or "g" on the first letter of this line for the generating Monkhorst-Pack. The forth line is for indicating the number of divisions in each direction of reciprocal unit cell. The fifth line specifies an additional shift of the k-mesh.

**POSCAR** indicates the size of the periodic boundary condition in three dimensions and both position and type of atom in the periodic boundary condition. One of POSCAR file of the first model of random placement method is shown below.

---

```
Amorphous_carbon
1.0
  8.7268    0.0000    0.0000
  0.0000    8.7268    0.0000
  0.0000    0.0000    8.7268
Amorphous_carbon
100
Direct
  0.1000    0.1000    0.1000
  0.1000    0.1000    0.3000
  0.1000    0.1000    0.5000
  0.1000    0.1000    0.7000
  0.1000    0.1000    0.9000
  0.1000    0.3000    0.1000
  0.1000    0.3000    0.3000
  0.1000    0.3000    0.5000
  0.1000    0.3000    0.9000
  0.1000    0.5000    0.1000
  0.1000    0.5000    0.3000
  0.1000    0.5000    0.5000
  0.1000    0.5000    0.7000
  0.1000    0.5000    0.9000
  0.1000    0.7000    0.1000
  0.1000    0.7000    0.5000
  0.1000    0.7000    0.9000
  0.1000    0.9000    0.1000
  0.1000    0.9000    0.3000
  0.1000    0.9000    0.5000
  0.1000    0.9000    0.7000
  0.3000    0.1000    0.1000
  0.3000    0.1000    0.5000
  0.3000    0.1000    0.7000
  0.3000    0.1000    0.9000
  0.3000    0.3000    0.3000
  0.3000    0.3000    0.5000
  0.3000    0.3000    0.7000
  0.3000    0.5000    0.1000
  0.3000    0.5000    0.3000
  0.3000    0.5000    0.5000
  0.3000    0.5000    0.7000
```

0.3000	0.7000	0.3000
0.3000	0.7000	0.5000
0.3000	0.7000	0.9000
0.3000	0.9000	0.1000
0.3000	0.9000	0.3000
0.3000	0.9000	0.5000
0.3000	0.9000	0.7000
0.5000	0.1000	0.1000
0.5000	0.1000	0.3000
0.5000	0.1000	0.5000
0.5000	0.1000	0.7000
0.5000	0.1000	0.9000
0.5000	0.3000	0.1000
0.5000	0.3000	0.7000
0.5000	0.3000	0.9000
0.5000	0.5000	0.1000
0.5000	0.5000	0.3000
0.5000	0.5000	0.5000
0.5000	0.5000	0.7000
0.5000	0.5000	0.9000
0.5000	0.7000	0.3000
0.5000	0.7000	0.7000
0.5000	0.7000	0.9000
0.5000	0.9000	0.1000
0.5000	0.9000	0.3000
0.5000	0.9000	0.7000
0.7000	0.1000	0.1000
0.7000	0.1000	0.5000
0.7000	0.1000	0.7000
0.7000	0.1000	0.9000
0.7000	0.3000	0.1000
0.7000	0.3000	0.3000
0.7000	0.3000	0.7000
0.7000	0.3000	0.9000
0.7000	0.5000	0.1000
0.7000	0.5000	0.3000
0.7000	0.5000	0.5000
0.7000	0.5000	0.9000
0.7000	0.7000	0.1000
0.7000	0.7000	0.7000
0.7000	0.9000	0.1000
0.7000	0.9000	0.3000
0.7000	0.9000	0.5000
0.7000	0.9000	0.7000
0.7000	0.9000	0.9000
0.9000	0.1000	0.1000
0.9000	0.1000	0.3000
0.9000	0.1000	0.5000

0.9000	0.1000	0.7000
0.9000	0.1000	0.9000
0.9000	0.3000	0.1000
0.9000	0.3000	0.3000
0.9000	0.3000	0.5000
0.9000	0.3000	0.7000
0.9000	0.3000	0.9000
0.9000	0.5000	0.1000
0.9000	0.5000	0.3000
0.9000	0.5000	0.9000
0.9000	0.7000	0.1000
0.9000	0.7000	0.3000
0.9000	0.7000	0.5000
0.9000	0.7000	0.7000
0.9000	0.7000	0.9000
0.9000	0.9000	0.1000
0.9000	0.9000	0.3000
0.9000	0.9000	0.5000
0.9000	0.9000	0.7000
0.9000	0.9000	0.9000

---

The first line indicates the name of this input file. The second line is the ratio of the lengths. Three lines from the third line are the vectors to indicate the periodic boundary condition. Each vector is in each line. The sixth line is the name of this structure. The seventh line is the amount of atoms in this structure. The eighth line is to indicate type for positioning each atom in this file. One is "Cartesian" or "Car" for positioning by actual number in the Cartesian coordinates. Another one is "Direct" for positioning by fraction of the length. The ninth line and below are the position of each atom.

**POTCAR** includes pseudo potential data of each type of atom in simulation. In this work, Projector Augmented Wave – Perdew-Burke-Ernzerhof (PAW-PBE) was performed for all simulations.

**OUTCAR** collects the input information from INCAR, POSCAR, and POTCAR file and also saves all calculated data of each ionic step such as ground energy and volume of cell that can determine the structure density.

**OSZICAR** collects the ground energy of current ionic step of which is a part the OUTCAR file. The OSZICAR file of the first model is shown in the following

---

	N	E	dE	d eps	ncg	rms	rms(c)
DAV: 1	0.185980186878E+04	0.18598E+04	-0.22810E+05	31856	0.170E+03		
DAV: 2	-0.689088151496E+03	-0.25489E+04	-0.24178E+04	39500	0.328E+02		
DAV: 3	-0.866113681271E+03	-0.17703E+03	-0.17132E+03	36816	0.837E+01		
DAV: 4	-0.871868244974E+03	-0.57546E+01	-0.57088E+01	39328	0.149E+01		
DAV: 5	-0.872051831657E+03	-0.18359E+00	-0.18326E+00	39056	0.262E+00	0.377E+01	
DAV: 6	-0.831572532908E+03	0.40479E+02	-0.45163E+01	34760	0.171E+01	0.205E+01	
DAV: 7	-0.823117732772E+03	0.84548E+01	-0.29508E+01	36776	0.135E+01	0.104E+01	
DAV: 8	-0.820504291250E+03	0.26134E+01	-0.97026E+00	34976	0.793E+00	0.316E+00	
DAV: 9	-0.820616555051E+03	-0.11226E+00	-0.18777E+00	35424	0.300E+00	0.205E+00	
DAV: 10	-0.820605533593E+03	0.11021E-01	-0.22283E-01	36280	0.121E+00	0.116E+00	
DAV: 11	-0.820610626277E+03	-0.50927E-02	-0.57937E-02	36240	0.636E-01	0.525E-01	
.							
.							
DAV: 9	-0.841455892957E+03	0.13806E-08	-0.23777E-07	36664	0.131E-03	0.811E-04	
DAV: 10	-0.841455892961E+03	-0.38581E-08	-0.83595E-08	35752	0.707E-04		
99 F=	-0.84145589E+03	E0= -0.84145589E+03	d E =-.923361E-02				
	N	E	dE	d eps	ncg	rms	rms(c)
DAV: 1	-0.841458073179E+03	-0.21802E-02	-0.47599E-02	32360	0.495E-01	0.477E-02	
DAV: 2	-0.841458103641E+03	-0.30462E-04	-0.90531E-04	37328	0.668E-02	0.346E-02	
DAV: 3	-0.841458091708E+03	0.11933E-04	-0.70875E-05	36584	0.214E-02	0.222E-02	
DAV: 4	-0.841458085621E+03	0.60865E-05	-0.22564E-05	35584	0.123E-02	0.109E-02	
DAV: 5	-0.841458084601E+03	0.10208E-05	-0.76639E-06	36592	0.731E-03	0.410E-03	
DAV: 6	-0.841458084439E+03	0.16177E-06	-0.16067E-06	36080	0.322E-03	0.180E-03	
DAV: 7	-0.841458084444E+03	-0.48021E-08	-0.32137E-07	35912	0.127E-03	0.909E-04	
DAV: 8	-0.841458084455E+03	-0.11501E-07	-0.42693E-08	27216	0.505E-04	0.401E-04	
DAV: 9	-0.841458084462E+03	-0.72414E-08	-0.98601E-09	18576	0.268E-04		
100 F=	-0.84145808E+03	E0= -0.84145808E+03	d E =-.219150E-02				

---

This OSZICAR file was written by 100 ionic steps' simulation that its number is shown in front of "F". In each ionic step, there are several electronic steps in the column "N". Column "E" is the current free energy. Column "dE" is the differences of between the current free energy and the last one. Column "d eps" is the differences of the bandstructure energies. Column "ncg" is the number of evaluations of the Hamiltonian acting onto a wavefunction. Column "rms" is the norm of the residuum of trial wavefunctions. Column "rms (c)" is the difference between input and output charge density.

The last line of each ionic step includes: "F" is the total free energy, "E0" is the energy when sigma becomes zero, and dE is the differences of free energies between the current step and the last step.

**CONTCAR** is written in the same format with the POSCAR file when the simulation has finished each ionic step and the simulation have already done. It includes the updated vectors of the periodic boundary condition and the updated positions of atoms.

### **3.3 Visualization**

The Open Visualization Tool (OVITO) is a free visualization software. OVITO has been developed by Alexander Stukowski, a postdoctoral at the Institute of Material Science at Darmstadt University of Technology, Germany. It can visualize and analyze the output file from molecular simulation including LAMMPS, XYZ, CFG, IMD, and POSCAR.

Since the CONTCAR file has the same format with the POSCAR file, it was analyzed by using OVITO to determine RDF of each simulation and the bond order of each carbon atom. *Figure 8* shows the appearance of OVITO evaluating the bond order of the first model of amorphous carbon created by the random placement method. Five functions were applied for each CONTCAR file: Wrap at periodic boundaries to limit the boundaries of the structure, Create bonds to generate bonds by setting cutoff radius at 1.8 Å, Coordination analysis to generate the RDF, Color coding to indicate the color of the bond order which the  $sp^1$  is blue,  $sp^2$  is green, and  $sp^3$  is red, and Histogram to count the amount of each bond order.

OVITO is capable to render the pictures of amorphous carbon structure that isotropic view was generated for each structure. In this work, the rendering engine was Tachyon renderer which the render parameters can be specified. The width and height of the picture were 1024 and 768 pixels, respectively. *Figure 9* shows the rendered picture of the first final amorphous carbon structure created by the random placement method. To render the better picture, the extra settings were set in the following:

Enable anti-aliasing	:	Yes
Anti-aliasing sample	:	20
Direct light	:	Yes
Brightness	:	0.9
Shadow	:	Yes
Ambient occlusion	:	Yes
Brightness	:	0.7
Sample count	:	30

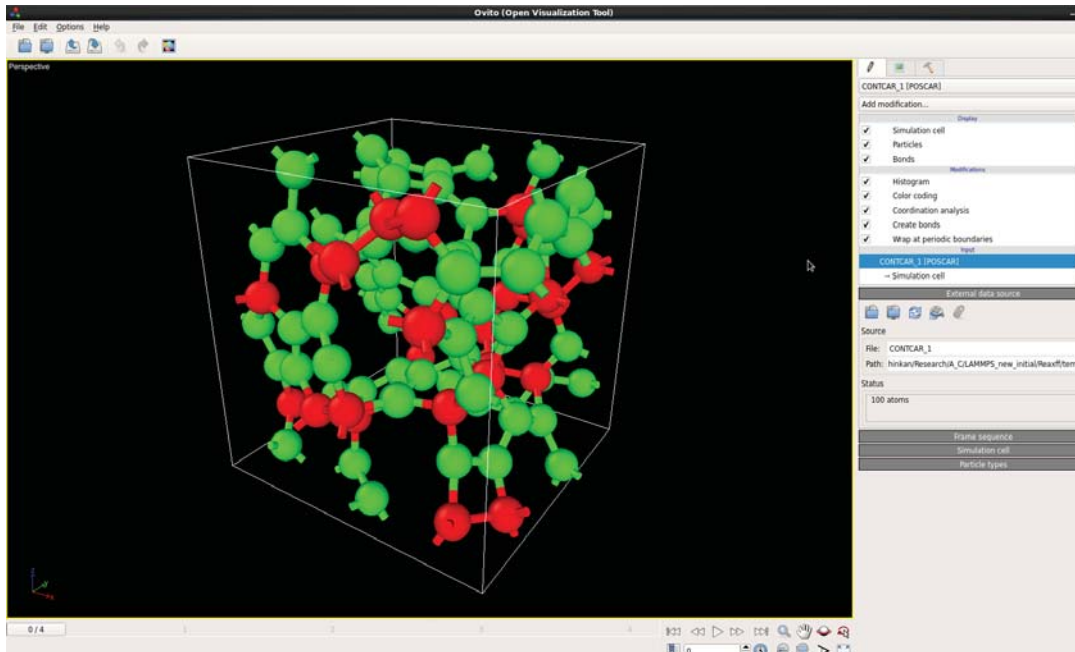


*Figure 8 The appearance of OVITO analyzing the first model of amorphous carbon created by the random placement method*



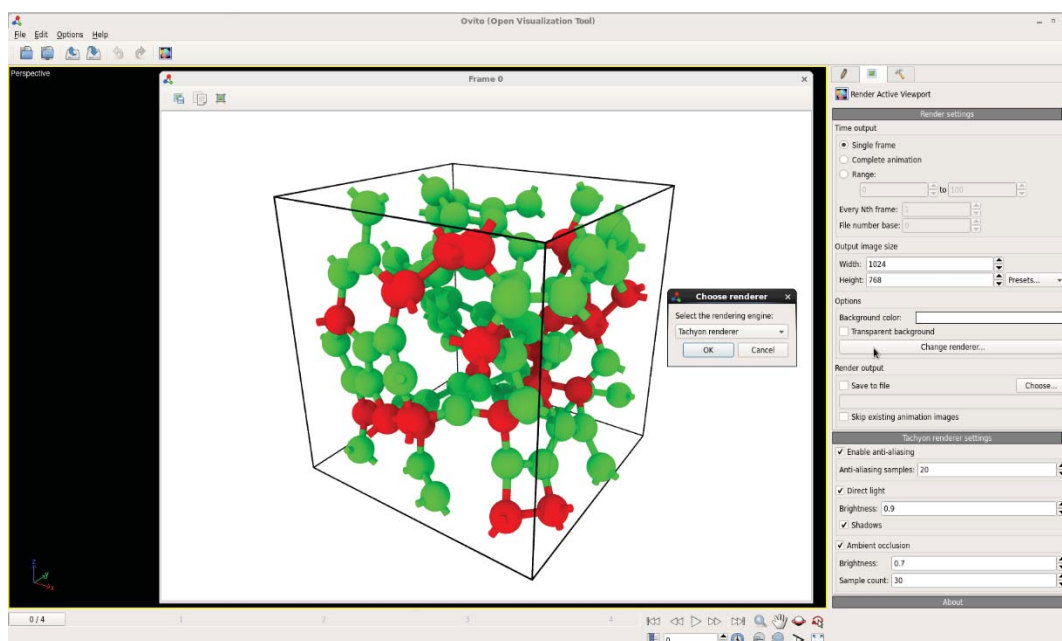


*Figure 9 The rendering process of OVITO analyzing the first model of amorphous carbon structure created by the random placement method*

## Chapter 4: Results and Discussion

### 4.1 Density

After optimizing amorphous carbon structures by using DFT in VASP, the density of each simulation is shown in *Figure 10*. The average density of the random placement method is equal to 2.59 g/cm<sup>3</sup>. This is more than the average density of the liquid-quench method, which is equal to 2.44 g/cm<sup>3</sup>. The standard deviations are 0.09 g/cm<sup>3</sup> and 0.07 g/cm<sup>3</sup>, respectively. Appendix A shows how to calculate the standard deviations.

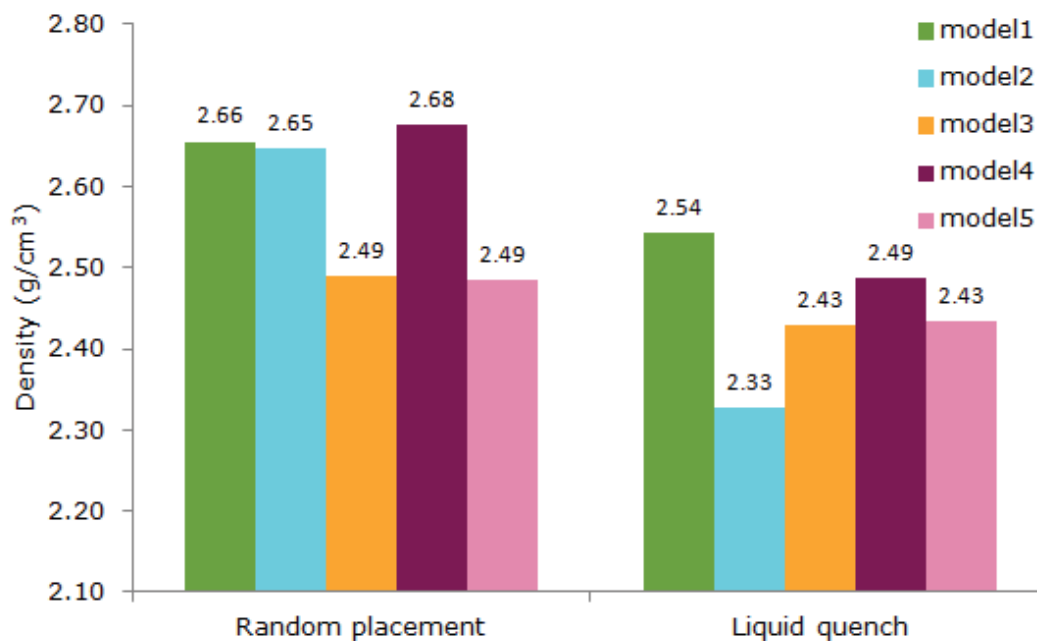


*Figure 10 Shown the densities of amorphous carbon structures created by the random placement method and the liquid-quench method*

## 4.2 Structure analysis

The RDF plot of the final amorphous carbon structures created by the random placement method is shown in *Figure 11*. Five models show  $G(r)$  with the same trends. The cutoff radius determined in this plot was 1.8 Å. Then, the cutoff radius was used to estimate the bond order of each final amorphous carbon structure shown in *Figure 12 to 16* that include blue, green, and red color of atoms to define the  $sp^1$ ,  $sp^2$ , and  $sp^3$  bonding, respectively.

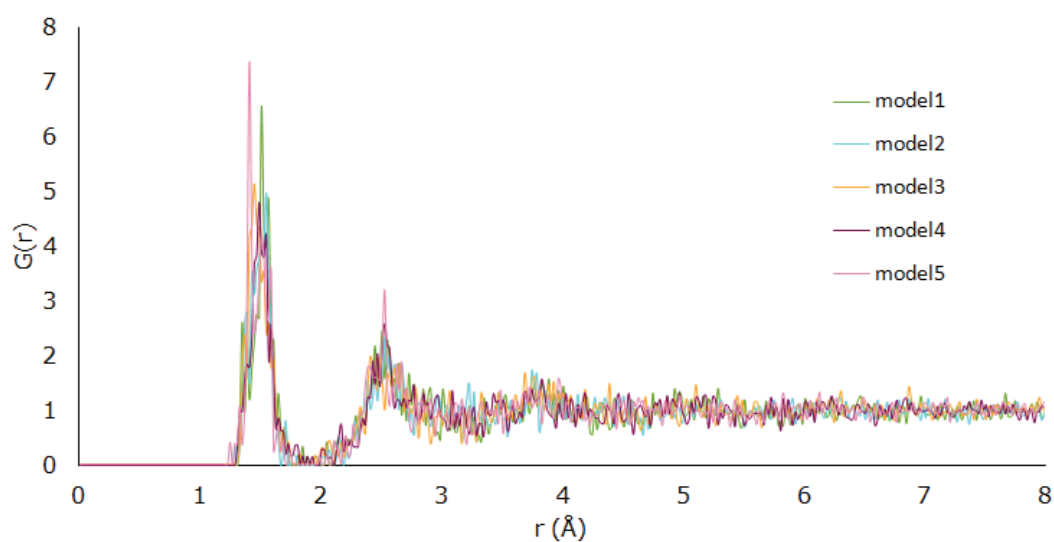


*Figure 11 The RDF plot of each final model of amorphous carbon created by the random placement method*

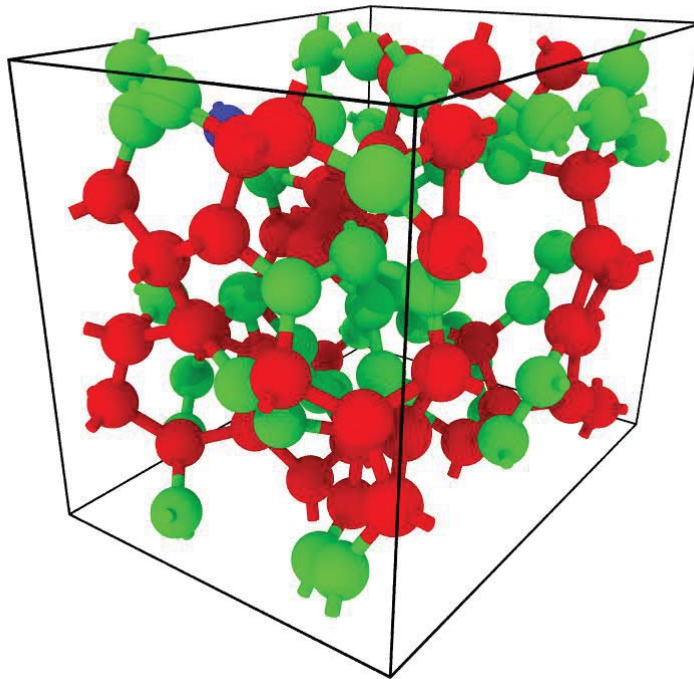


*Figure 12 Shown the bond order of the first final amorphous carbon model created by the random placement method with  $sp^3$  bonded atom red,  $sp^2$  areen and  $sp$  blue*

*Figure 12* shows the bond order of the first final amorphous carbon structure by the random placement method. The percentage of the  $sp^1$ ,  $sp^2$ , and  $sp^3$  bonding are 1%, 52%, and 47%, respectively.

*Figure 13* shows the bond order of the second final amorphous carbon structure by the random placement method. There is no the  $sp^1$  bonding in this result so the percentage of the  $sp^2$  and  $sp^3$  bonding are 60%, and 40%, respectively.

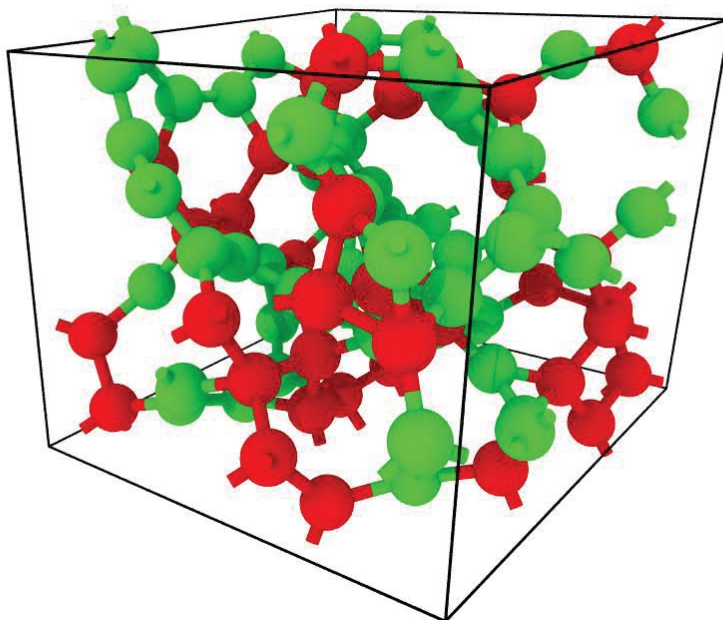


*Figure 13 shown the bond order of the second final amorphous carbon model created by the random placement method with  $sp^3$  bonded atom red and  $sp^2$  green*

*Figure 14 shows the bond order of the third final amorphous carbon structure by the random placement method. The percentage of the  $sp^1$ ,  $sp^2$ , and  $sp^3$  bonding are 1%, 66%, and 33%, respectively.*

*Figure 15 shows the bond order of the fourth final amorphous carbon structure by the random placement method. There is no the  $sp^1$  bonding in this result so the percentage of the  $sp^2$  and  $sp^3$  bonding are 60% and 40%, respectively.*

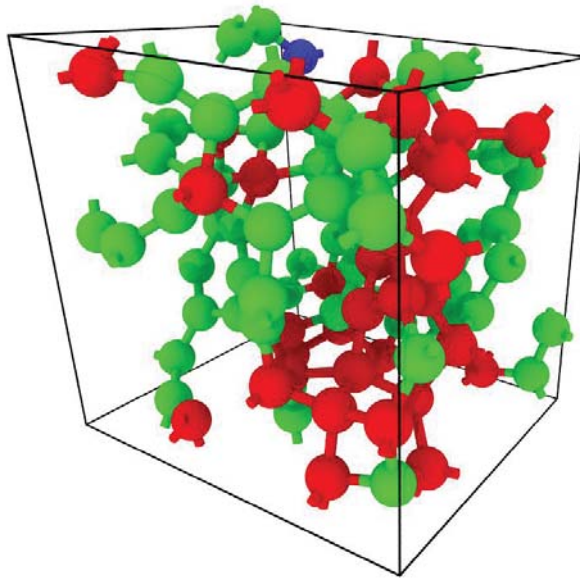


*Figure 15 shown the bond order of the forth final amorphous carbon model created by the random placement method with  $sp^3$  bonded atom red,  $sp^2$  green and  $sp$  blue*

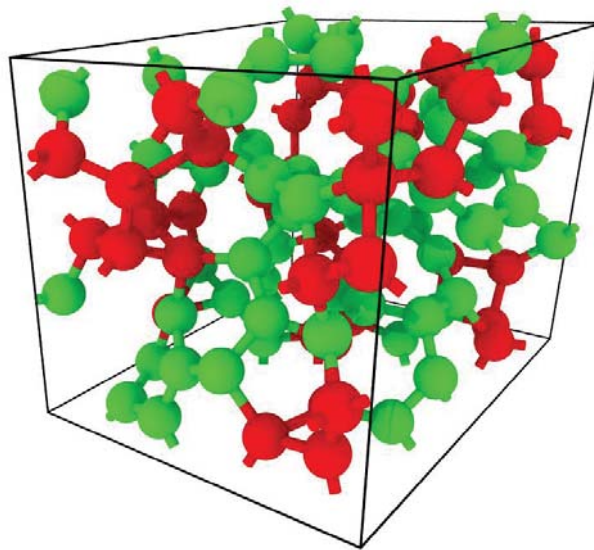


*Figure 14 shown the bond order of the third final amorphous carbon model created by the random placement method with  $sp^3$  bonded atom red and  $sp^2$  green*

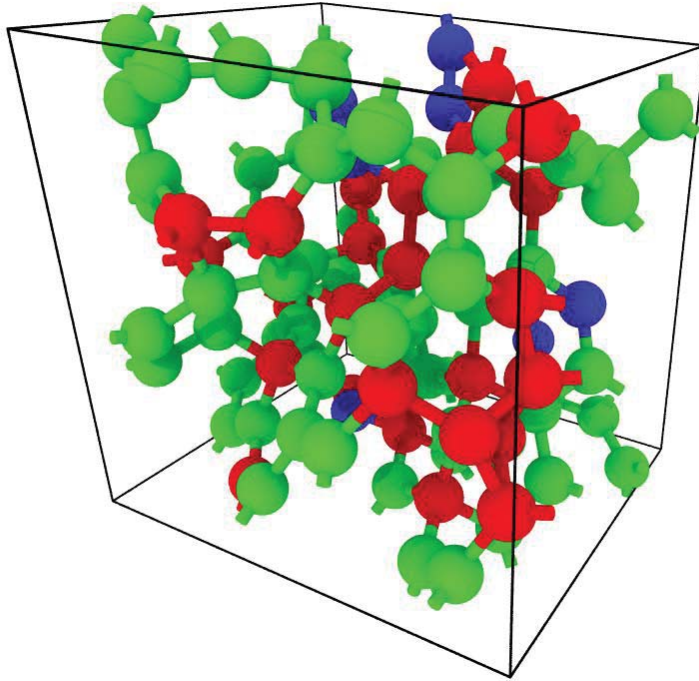


*Figure 16 shown the bond order of the fifth final amorphous carbon model created by the random placement method with  $sp^3$  bonded atom red,  $sp^2$  green and  $sp$  blue*

*Figure 16 shows the bond order of the fifth final amorphous carbon structure by the random placement method. The percentage of the  $sp^1$ ,  $sp^2$ , and  $sp^3$  bonding are 7%, 68%, and 25%, respectively.*

In *Figure 17*, the RDF plot of the final amorphous carbon structures created by the liquid-quench method is shown. Five models have  $G(r)$  same trend. The cutoff radius determined in this plot was also 1.8 Å. Then, the cutoff radius was used to estimate the bond order of each final amorphous carbon structure shown in *Figure 18* to *22*.

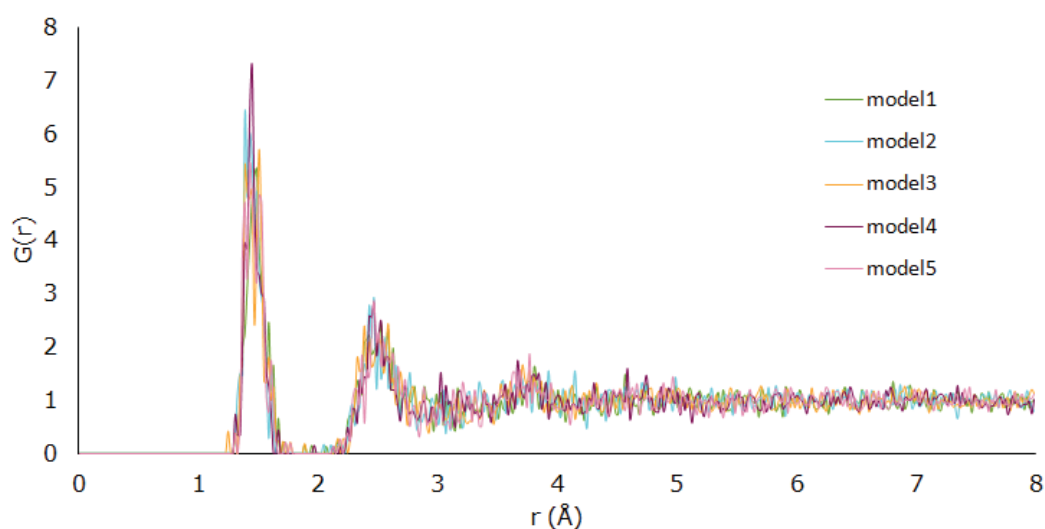
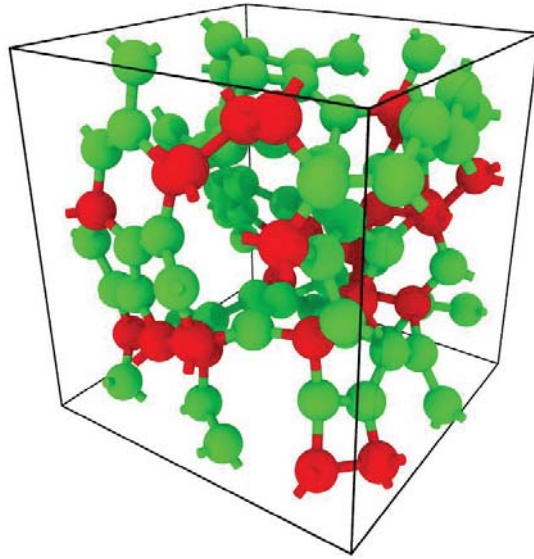


*Figure 17* shown the RDF plot of each final model of amorphous carbon created by the liquid-quench method

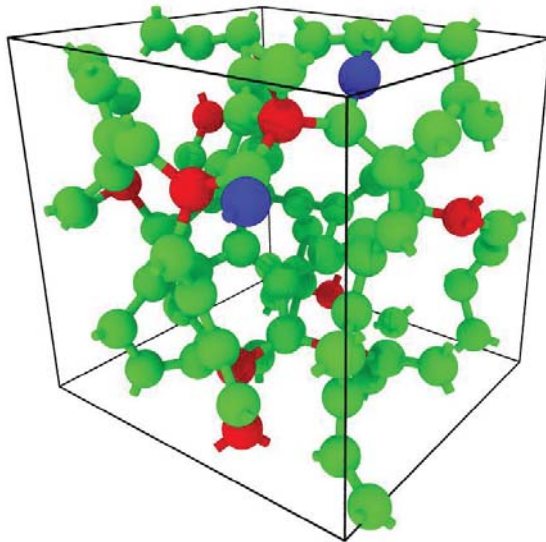
*Figure 18* shows the bond order of the first final amorphous carbon structure by the liquid-quench method. There is no the  $sp^1$  bonding in this result so the percentage of the  $sp^2$  and  $sp^3$  bonding are 72% and 28%, respectively.

*Figure 19* shows the bond order of the second final amorphous carbon structure by the liquid-quench method. The percentage of the  $sp^1$ ,  $sp^2$ , and  $sp^3$  bonding are 2%, 88%, and 10%, respectively.



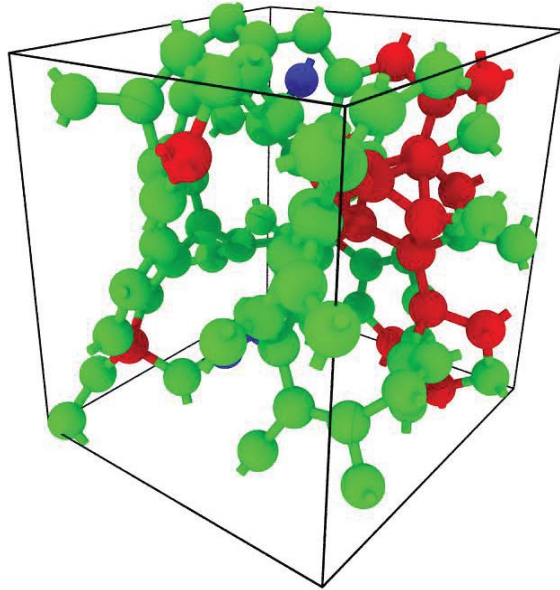


*Figure 18 shown the bond order of the first final amorphous carbon model created by the liquid-quench method with  $sp^3$  bonded atom red and  $sp^2$  green*



*Figure 19 shown the bond order of the second final amorphous carbon model created by the liquid-quench method with  $sp^3$  bonded atom red,  $sp^2$  green and  $sp$  blue*

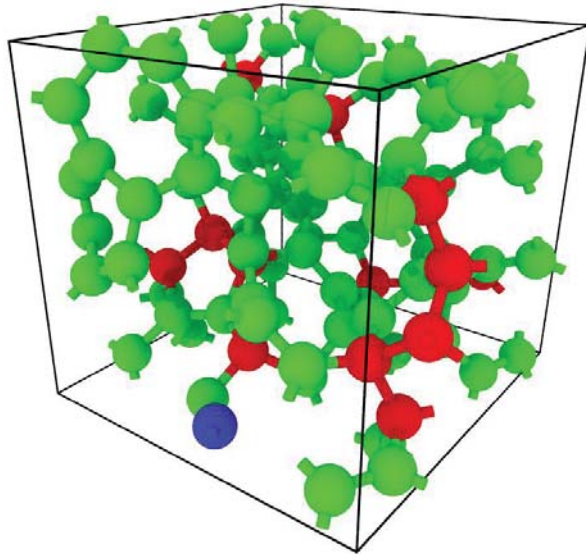
Figure 20 shows the bond order of the third final amorphous carbon structure by the liquid-quench method. The percentage of the  $sp^1$ ,  $sp^2$ , and  $sp^3$  bonding are 3%, 76%, and 21%, respectively.



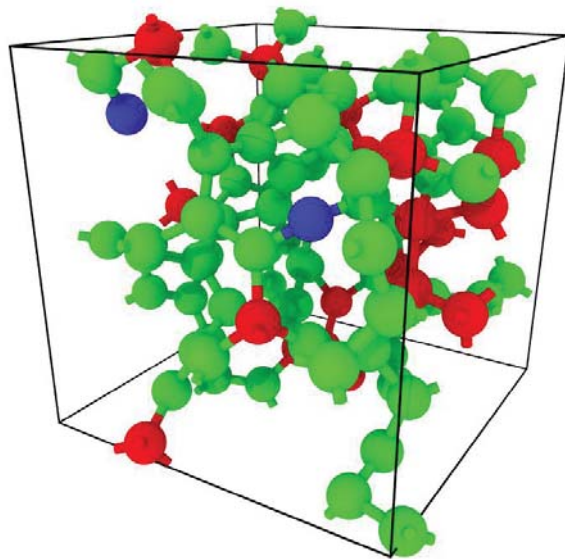
*Figure 20 shown the bond order of the third final amorphous carbon model created by the liquid-quench method with  $sp^3$  bonded atom red,  $sp^2$  green and  $sp$  blue*

Figure 21 shows the bond order of the fourth final amorphous carbon structure by the liquid-quench method. The percentage of the  $sp^1$ ,  $sp^2$ , and  $sp^3$  bonding are 1%, 86%, and 13%, respectively.

Figure 22 shows the bond order of the fifth final amorphous carbon structure by the liquid-quench method. The percentage of the  $sp^1$ ,  $sp^2$ , and  $sp^3$  bonding are 2%, 78%, and 20%, respectively.



*Figure 21 shown the bond order of the fourth final amorphous carbon model created by the liquid-quench method with  $sp^3$  bonded atom red,  $sp^2$  green and  $sp$  blue*



*Figure 22 shown the bond order of the fifth final amorphous carbon model created by the liquid-quench method with  $sp^3$  bonded atom red,  $sp^2$  green and  $sp$  blue*

Figure 23 shows the average percentage of each bonding order. The average percentage of the  $sp^1$  bonding of both methods are the same. The average  $sp^2$  percentage of the liquid-quench method is higher than the average  $sp^2$  percentage of the random placement method. In contrast, the average  $sp^3$  percentage of the liquid-quench method is lower than the average  $sp^3$  percentage of the random placement method.

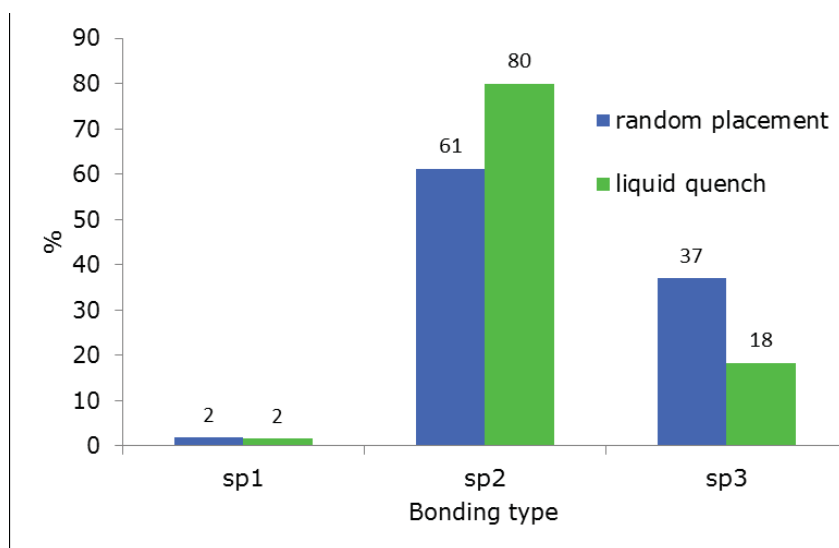


Figure 23 shown the average percentages of each bond order of the final amorphous carbon models by using OVITO

Amorphous carbon normally consists of the  $sp^2$  and  $sp^3$  bonding. If amorphous carbon has the higher fraction of  $sp^3$ , its properties tend to be similar to some mechanical properties of diamond. The fraction of  $sp^3$  bonding of amorphous carbon has been investigated; many research projects studied this important  $sp^3$  fraction.

Figure 24 shows that the average  $sp^3$  percentages of amorphous carbon determined by OVITO are lower than the average  $sp^3$  percentages of amorphous carbon calculated by Equation 1.

Since DFT was performed to determine the lowest energy of the amorphous carbon structures and the  $sp^2$  bonding is more stable than the  $sp^3$  bonding, the  $sp^2$  fractions of the amorphous carbon structures in this work tend to be higher. Consequently, the  $sp^3$  fractions of the amorphous carbon structures tend to be lower.

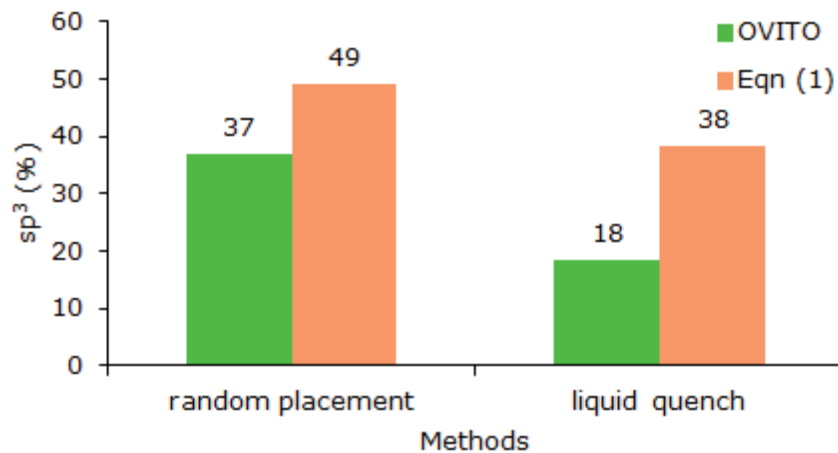
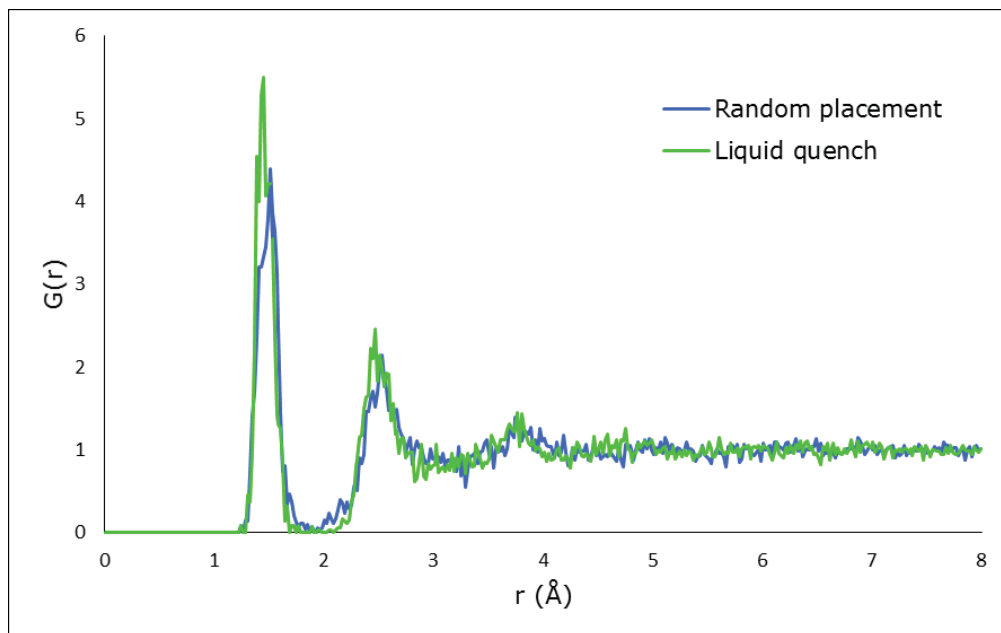


Figure 24 compared the average  $sp^3$  percentage of amorphous carbon created by both methods using OVITO and Equation 1



*Figure 25 compared average RDF of amorphous carbon structure created by the random placement method and the liquid-quench method*

Figure 25 shows the comparison of RDF of amorphous carbon structure created by the random placement method and the liquid-quench method that they are almost the same. At the first peak, the amorphous carbon created by the liquid-quench method has higher number of atoms. It means this method can generate the structure of amorphous carbon that is denser than another method. This is in good agree with the result that the amorphous carbon structure created by the liquid-quench method has more sp<sup>2</sup> bonding that the bond length is shorter than the sp<sup>3</sup> bonding.

### 4.3 Energy analysis

Since the simulations were run with an ionic step of 100, the ground-state energy of amorphous carbon systems were dependent on the initial structures. *Figure 26* shows the ground energies of the random placement method and the liquid-quench method changing by the ionic step.

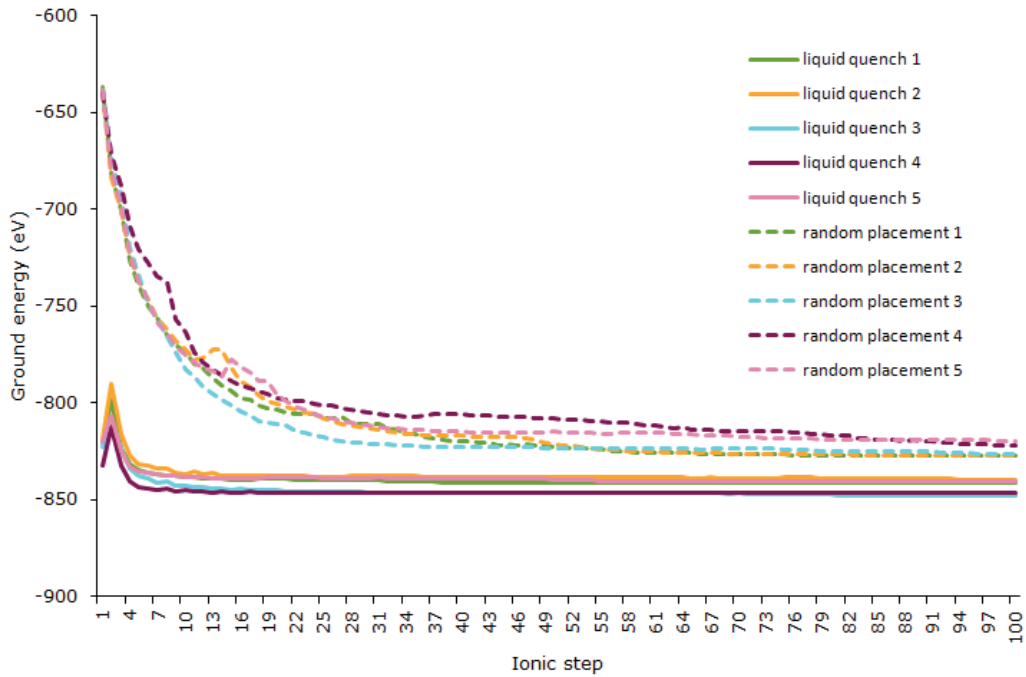


*Figure 26 shown the ground-state energies of amorphous carbon structure generated by both methods changing by the ionic step*

The final ground-state energies of each amorphous carbon structure approach the same range. The final ground-state energies of amorphous carbon structures created by the liquid-quench method are lower than the final ground energies of amorphous carbon structures created by the random placement method. The average final ground energies of amorphous carbon structures created by the

random placement method and the liquid-quench method are -824.61 and -843.42 eV, respectively.

Since the peaks of the ground energy of the amorphous carbon structure created by the liquid-quench method appear in *Figure 26*, they are interesting data. To see more of the details when the structure was changing, the densities of amorphous carbon structures created by both methods were plotted with the ionic step shown in *Figure 27*.

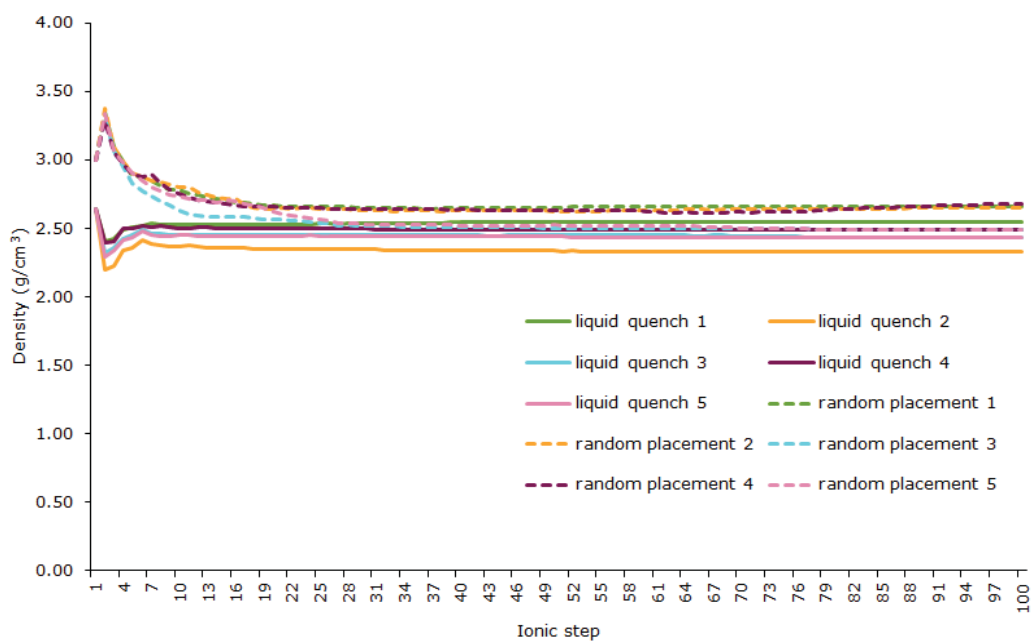


*Figure 27* shown the densities of amorphous carbon structure generated by both methods changing by the ionic step

For the liquid-quench method, the peaks might indicate that the carbon atoms of the initial structure were too close to each other so they attempted to relax and



expand the structures. Consequently, the ground energies at this ionic step dropped as shown in *Figure 26*.

For the densities of the random placement method in *Figure 27*, there are the peaks of the densities at the beginning. Because the initial structures of amorphous carbon were like the lattices with few spaces, each carbon atom moved closer and approached to the other carbon atom. The structures became too tight so they tried to refine the positions of the carbon atoms to a stable state.

## **Chapter 5: Conclusion**

The average densities of amorphous carbon created by the random placement method and the liquid-quench method are 2.59 and 2.44 g/cm<sup>3</sup> with standard deviations of 0.09 and 0.07 g/cm<sup>3</sup>, respectively. These densities are the middle range of the densities from the previous literatures shown in *Table 4*.

The experimental densities of amorphous carbon in *Table 4* were varied. The lower densities might be obtained from the specimens that were consisted of the void. On the other hand, the higher densities of amorphous carbon were determined from the tetrahedral amorphous carbon or the diamond-like carbon that has a density that is close to the diamond density.

The computational results in *Table 4* show that the densities of the amorphous carbon tended to be extremely high densities. Because the ground energy of these amorphous carbon structures might not be the lowest energy, the structures were squeezed to be similar to the tetrahedral amorphous carbon or the diamond-like carbon structures that had densities that were very high.

The difference between the random placement method and the liquid-quench method is that the average ground energy of the liquid-quench method is lower than the average ground energy of the random placement. The liquid-quench method with the ReaxFF and DFT has a greater ability to minimize the energy and refine the position.

In conclusion, the combination of the ReaxFF and DFT (liquid-quench method) can predict the density of amorphous carbon at the lowest ground energy. This density is the actual density of amorphous carbon without the external force, so it can be implemented for modeling the materials, including the amorphous carbon, such as the carbon nanotubes composite materials.

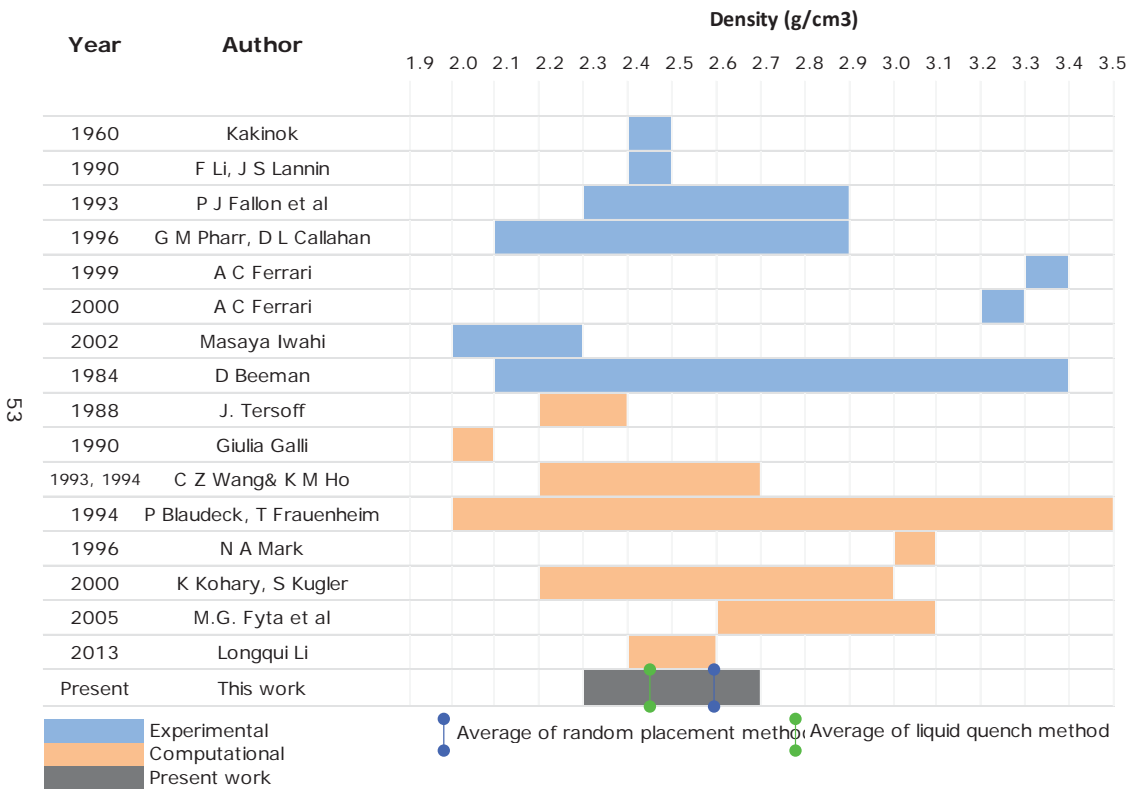


Table 4 shown the comparison the densities between this present work and the previous literatures

## Chapter 6: References

1. Education TJNAF-OoS. 2014 The Element Carbon.  
<<http://education.jlab.org/itselemental/ele006.html>>.
2. Novoselov KS, Geim AK, Morozov SV, Jiang D, Zhang Y, Dubonos SV, Grigorieva IV, Firsov AA. Electric field effect in atomically thin carbon films. *Science* 2004;306(5696):666-669.
3. Kakinoki J, Komura Y, Ino T. Electron diffraction study of evaporated carbon films. *Acta Crystallographica* 1960;13(3):171-179.
4. Boiko BTP, L. S.; Derevyanchenko, A. S. Structure of Amorphous Carbon Films. *Soviet Physics Doklady* 1968;13:237.
5. Beeman D, Silverman J, Lynds R, Anderson M. Modeling studies of amorphous carbon. *Physical Review B* 1984;30(2):870-875.
6. Li F, Lannin J. Radial distribution function of amorphous carbon. *Physical Review Letters* 1990;65(15):1905-1908.
7. Fallon P, Veerasamy V, Davis C, Robertson J, Amaratunga G, Milne W, Koskinen J. Properties of filtered-ion-beam-deposited diamondlike carbon as a function of ion energy. *Physical Review B* 1993;48(7):4777-4782.
8. Pharr GM, Callahan DL, McAdams SD, Tsui TY, Anders S, Anders A, Ager JW, Brown IG, Bhatia CS, Silva SRP and others. Hardness, elastic modulus, and structure of very hard carbon films produced by cathodic-arc deposition with substrate pulse biasing. *Applied Physics Letters* 1996;68(6):779.
9. Ferrari AC, Robertson J, Beghi MG, Bottani CE, Ferulano R, Pastorelli R. Elastic constants of tetrahedral amorphous carbon films by surface Brillouin scattering. *Applied Physics Letters* 1999;75(13):1893-1895.
10. Ferrari AC, Kleinsorge B, Adamopoulos G, Robertson J, Milne WI, V S, Brown LM, LiBassi A, Tanner BK. Determination of bonding in amorphous carbons by electron energy loss spectroscopy, Raman scattering and X-ray reflectivity. *Journal of Non-Crystalline Solids* 2000;266:765-768.
11. Iwaki M. Estimation of the atomic density of amorphous carbon using ion implantation, SIMS and RBS. *Surface & Coatings Technology* 2002;158:377-381.
12. Tersoff J. Empirical Interatomic Potential for Carbon, with Applications to Amorphous Carbon. *Physical Review Letters* 1988;61(25):2879-2882.
13. Robertson J. Amorphous carbon. *Advances in Physics* 1986;35(4):317-374.
14. Galli G, Martin RM, Parrinello M. Ab initio calculation of properties of carbon in the amorphous and liquid states. *Physical Review B* 1990;42(12):7470-7482.
15. Wang C, Ho K, Chan C. Tight-binding molecular-dynamics study of amorphous carbon. *Physical Review Letters* 1993;70(5):611-614.
16. Wang CZ, Ho KM. The Electronic-Structure of Diamond-Like Amorphous-Carbon. *Journal of Physics-Condensed Matter* 1994;6(17):L239-L244.

17. Marks NA, McKenzie DR, Pailthorpe BA, Bernasconi M, Parrinello M. Microscopic structure of tetrahedral amorphous carbon. *Physical Review Letters* 1996;76(5):768-771.
18. Kohary K, Kugler S. Time development during growth and relaxation of amorphous carbon films. Tight-binding molecular dynamics study. *Journal of non-crystalline solids* 2002;299:824-829.
19. Fyta MG, Mathioudakis C, Kopidakis G, Kelires PC. Structure, stability, and stress properties of amorphous and nanostructured carbon films. *Thin Solid Films* 2005;482(1):56-62.
20. Li L, Xu M, Song W, Ovcharenko A, Zhang G, Jia D. The effect of empirical potential functions on modeling of amorphous carbon using molecular dynamics method. *Applied Surface Science* 2013;286:287-297.
21. Van Duin AC, Dasgupta S, Lorant F, Goddard WA. ReaxFF: a reactive force field for hydrocarbons. *The Journal of Physical Chemistry A* 2001;105(41):9396-9409.
22. Sholl DS, Steckel JA. *Density functional theory : a practical introduction*. Hoboken, N.J.: Wiley; 2009. xii, 238 p. p.
23. Perdew JP, Zunger A. Self-Interaction Correction to Density-Functional Approximations for Many-Electron Systems. *Physical Review B* 1981;23(10):5048-5079.
24. Perdew JP, Chevary JA, Vosko SH, Jackson KA, Pederson MR, Singh DJ, Fiolhais C. Atoms, Molecules, Solids, and Surfaces - Applications of the Generalized Gradient Approximation for Exchange and Correlation. *Physical Review B* 1992;46(11):6671-6687.
25. Perdew JP, Chevary JA, Vosko SH, Jackson KA, Pederson MR, Singh DJ, Fiolhais C. Atoms, Molecules, Solids, and Surfaces - Applications of the Generalized Gradient Approximation for Exchange and Correlation (Vol 46, Pg 6671, 1992). *Physical Review B* 1993;48(7):4978-4978.
26. Perdew JP, Burke K, Ernzerhof M. Generalized gradient approximation made simple. *Physical Review Letters* 1996;77(18):3865-3868.
27. Perdew JP, Burke K, Ernzerhof M. Generalized gradient approximation made simple (vol 77, pg 3865, 1996). *Physical Review Letters* 1997;78(7):1396-1396.
28. Kresse G, Hafner J. Ab-initio Molecular-Dynamics for Liquid-Metals. *Physical Review B* 1993;47(1):558-561.
29. Kresse G, Hafner J. Ab-Initio Molecular-Dynamics Simulation of the Liquid-Metal Amorphous-Semiconductor Transition in Germanium. *Physical Review B* 1994;49(20):14251-14269.
30. Kresse G, Furthmuller J. Efficient iterative schemes for ab initio total-energy calculations using a plane-wave basis set. *Physical Review B* 1996;54(16):11169-11186.
31. Kresse G, Furthmuller J. Efficiency of ab-initio total energy calculations for metals and semiconductors using a plane-wave basis set. *Computational Materials Science* 1996;6(1):15-50.

## Appendix A

### A.1 Selection of Energy Cutoff and KPOINTS

To optimize the simulation time and have consistent results, the KPOINTS and the energy cutoff are needed to be selected by comparing the ground energies ( $E_0$ ) of amorphous carbon structure. The structure was frozen so that each atom cannot move and the boundaries are also fixed.

At the beginning, the KPOINTS was fixed at 5x5x5 but the energy cutoff was varied from 300 to 800 eV with increments of 50 eV. *Figure 29* shows the ground energies of amorphous carbon structure by changing the energy cutoff. Since the ground energy became stable when the energy cutoff was equal to and above 500 eV, the energy cutoff of 600 eV was selected to use in all simulations.

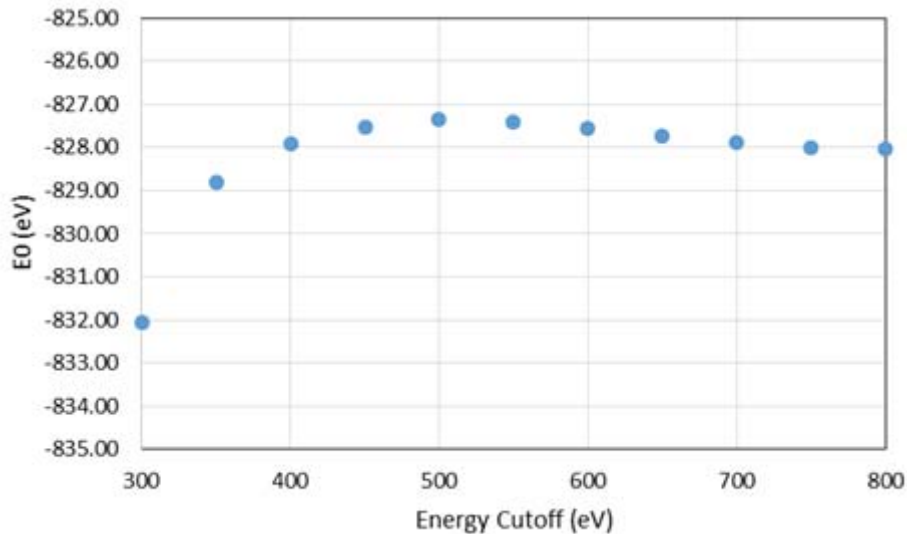


*Figure 28 compared the ground energies of amorphous carbon by changing energy cutoff variable*

Then, the energy cutoff was fixed to 600 eV but the KPOINTS was varied from 3 to 8 to run the simulation of amorphous carbon. *Table 5* shows the ground energies of amorphous carbon structure by varying the KPOINTS that all ground energies are the same. The KPOINTS of 5x5x5 was selected to apply to all simulations.

*Table 5 shown the ground energies of amorphous carbon structure by varying KPOINTS and energy cutoff*

KPOINTS	Energy Cutoff (eV)	E0 (eV)
5x5x5	300	-832.05
	350	-828.80
	400	-827.92
	450	-827.53
	500	-827.36
	550	-827.40
	600	-827.56
	650	-827.74
	700	-827.89
	750	-827.99
800	-828.04	
3x3x3	600	-827.55
4x4x4		-827.55
5x5x5		-827.56
6x6x6		-827.56
7x7x7		-827.56
8x8x8		-827.56
		-827.55



## **A.2 Calculation of the standard deviation**

In this section, the calculation of the standard deviation is shown by giving an example of the densities of amorphous carbon created by the random placement method. They are 2.66, 2.65, 2.49, 2.68, and 2.49 g/cm<sup>3</sup> that the average density is 2.59 g/cm<sup>3</sup>.

Standard deviation

$$= \sqrt{\frac{(2.66 - 2.59)^2 + (2.65 - 2.59)^2 + (2.49 - 2.59)^2 + (2.68 - 2.59)^2 + (2.49 - 2.59)^2}{5}}$$
$$= 0.09 \text{ g/cm}^3$$

The standard deviation of the densities of amorphous carbon created by the random placement method is 0.09 g/cm<sup>3</sup> as shown above. The standard deviation of the densities of amorphous carbon created by the liquid-quench method also used this method to determine. It is equal to 0.07 g/cm<sup>3</sup>.

## **Appendix B: Computer Commands**

### **B.1 Unix Command**

In this work, the terminal was performed to be like a bridge between the user and the computing cluster. It is necessary to know the command to edit the input file, to extract the data from the output file, to moving or copying the file to the other directory, to manage the files, to determine the basic calculation, and to communicate to the cluster. *Table 6* shows the description of the commands that were used in this research.

*Table 6 shown the unix commands used in this work*

cd (name of directory)	To change directory
Ls	To show the list of all files and folders.
mkdir (name of directory)	To create new folder or directory
rm -f (filename)	To remove file [-f define to force to remove]
rm -fr (folder name)	To remove folder and contents.
cp (source) (target)	To copy file to the other location (same computer)
rsync -avz (source) (target)	To copy file to the other location (different computers)
grep "(keyword)"	To search and print the line that has this keyword
vi (filename)	To edit the file
less (filename)	To see the file without editing
tail (filename)	To print the bottom part of file
head (filename)	To print the top part of file
awk -F'keyword' (filename)	To extract the part from file



## **B.2 Computing Cluster**

Superior is a central high performance computing cluster at Michigan Technological University. In this work, many simulations were submitted through this computing cluster by using the commands on the terminal. The user need to use these following commands.

### **Login**

1. Input this command "ssh -Y (user\_name)@superior-login1.research.mtu.edu".
2. Then, the user has to type in the password.

### **Logout**

1. Put this command "logout" or "exit".

### **Submission**

1. Put this command "qgenerate".
2. Select the software by putting the number of software from the software list.
3. Select queuing type by putting the name of queuing type from the list.
4. Put the commands by following the instruction.
5. Put this command "qsub (input/script file name)" for submitting the simulation.

### **Monitor**

1. Put this command "quser" to check the status of simulation.

## Appendix C: Input files of LAMMPS (ReaxFF)

### C.1 script.coords

```
variable          I equal ((100*12.011/(2.6*1.015*0.6022142))^(1/3))/2
region            simboxreg block -$I $I -$I $I -$I $I units box
create_box        1 simboxreg

create_atoms      1 random 100 759202135 NULL units box
mass              1 12.0
```

### C.2 Imp control

```
simulation_name   Amorphous_Carbon_2 ! output files will carry this name + their specific
ext

tabulate_long_range 10000 ! denotes the granularity of long range tabulation, 0 means no
tabulation
energy_update_freq 1

nbrhood_cutoff    4.5 ! near neighbors cutoff for bond calculations in A
hbond_cutoff       6.0 ! cutoff distance for hydrogen bond interactions
bond_graph_cutoff  0.3 ! bond strength cutoff for bond graphs
thb_cutoff         0.001 ! cutoff value for three body interactions

write_freq        1 ! write trajectory after so many steps
traj_title        Amor_C ! (no white spaces)
atom_info         1 ! 0: no atom info, 1: print basic atom info in the trajectory file
atom_forces       1 ! 0: basic atom format, 1: print force on each atom in the trajectory
file
atom_velocities   0 ! 0: basic atom format, 1: print the velocity of each atom in the
trajectory file
bond_info         1 ! 0: do not print bonds, 1: print bonds in the trajectory file
angle_info        1 ! 0: do not print angles, 1: print angles in the trajectory file
```

### **C.3 in.ac**

```
# REAX potential for CHO system
# .....

#-----Initialization-----
units      real
dimension  3
boundary   p p p
atom_style charge

#-----Geometry-----
include     script.coords

pair_style  reax/c Imp_control
pair_coeff  * *ffield.reax.Aug17 C
fix        chargeeq all qeq/reax 1 0.0 10.0 1.0e-6 reax/c

#-----Minimization-----
fix        1 all nve
fix        3 all temp/berendsen 5000.0 1.0 500.0

timestep   0.1

dump       1 all atom 1000 dump.reax.amorphous_2.carbon

run        100000
```